U.S. RESEARCH

4319

OPS

DOT-RSPA-DPB-50/81/4

Reliability of Ultrasonic Weld Interrogation Methods

JANUARY 1981

PHASE ONE REPORT
UNDER CONTRACT
DOT-RC-92014

Document is available to the U.S. public through
The National Technical Information Service,
Springfield, Virginia 22161

U.S. DEPARTMENT OF TRANSPORTATION
Research & Special Programs Administration
Office of University Research
Washington, D.C. 20590

NOTICE

This document is disseminated under the sponsorship of the Department of Transportation in the interest of information exchange. The United States Government assumes no liability for its contents or use thereof.

Technical Report Documentation Page

4. Title and Subtitle Reliability of Ultrasonic Weld Interrogation Methods	5. Report Date January 1981 6. Performing Organization Code
7. Author(s) Steven Serabian	8. Performing Organization Report No DOT-RC-92014,I
9. Performing Organization Name and Address University of Lowell One University Avenue Lowell, Massachusetts 01854	10. Work Unit No (TRAIS) 11. Contract or Grant No. DOT-RC-92014
	13. Type of Report and Period Covered Final Report - Phase I 29 June 1979 - 29 June 1980
	14. Sponsoring Agency Code DPB-50

16. Abstract

The report presents a critical review of the present state-of-the-art of the ultrasonic methods and procedures available for the nondestructive evaluation of weldments. The type of flaw considered was the planar - totally embedded reflector. Amplitude-dependent and amplitude-independent flaw characterization techniques are examined by theoretical and experimental means to assess detecting ability and reliability. Emphasis is given to flaw characterization in terms of location, size and orientation.

17. Key Words ultrasonic weld interrogation, flaw detection, flaw characterization, flaw size & orientation determinations.	18. Distribution Statement Document is available to the U.S. Public through the National Technical Information Service, Springfield, VA 22161

19. Security Classif. (of this report)	20. Security Classif. (of this page)	21. No. of Pages	22. Price
Unclassified	Unclassified	253	

Form DOT F 1700.7 (8-72)

TABLE OF CONTENTS

TABLE OF CONTENTS (Cont'd)

I. PREFACE

This report summarizes the salient points of the research activities of the first year of a two year program whose prime objectives are:

a. Critique the present state-of-the-art of the ultrasonic techniques and procedures used to assess weldment quality. Categorize each technique and procedure for effectiveness or reliability to characterize the detected flaw content - i.e., location, size, orientation and shape.

b. Based upon the results of the above critique, the most promising of the available techniques will be selected for further study and improvement. The chosen techniques will encompass data interpretation methods whose intelligence is derived from both amplitude-dependent and amplitude-independent considerations. This work will be accomplished with analytical modelling of the detection processes as well as experimental investigations involving simulated flaws in homogenious materials. Detection probabilities based upon flaw size, location and orientation will be generated. The influence of the weldment and base materials and the weld configuration will be evaluated.

c. Validate the reliabilities of selected techniques and procedures using natural weldment flaws. A detailed evaluation of the influence of flaw, material, instrumentation and weld design parameters responsible for the differences between actual and predicted results will be generated. Such assessments will be used to formulate and institute corrective measures to optimize the ultrasonic interrogation techniques involved.

The results of the first two items listed above constitute the study program of the first year and are reported herein. Item c represents the work to be performed during the second year of this program.

11. EXECUTIVE SUMMARY

Of all the material joining processes welding is the most desirable for critical structures. The advantages of welding are many and varied. For example, welding allows designs which have an aesthetic balance of form and proportion. Welded structures are more reliable, stronger and have less weight and waste as well as requiring less maintenance. The costs for welding tend to offset the increasing price of labor and materials. Moreover, in general, the inspection of weldments can be made in situ.

Present day designs have pushed materials/structures to the limits of their abilities. This has created a need for proven reliability. To this end, two different technologies are being used - i.e., fracture mechanics and nondestructive testing. In fracture mechanics one can relate stress, fracture toughness and flaw size. This has facilitated the determination of an acceptable flaw content for a structure subjected to a given operational environment. On the other hand, the objective of the nondestructive testing in this situation is to characterize the flaw content of a given material/structure in terms of those parameters necessary to interface with fracture mechanics - e.g., flaw size, location, orientation, and shape.

It is interesting to note that both fracture mechanics and the ultrasonic mode of evaluation were both generated about the same time. However, it becomes apparent, at even a cursory glance, that their growths have not been the same. Fracture mechanics has evolved into a major analysis technique and continues to make significant advances. However, ultrasonic procedures and techniques have not changed much since their advent. Advances have been primarily in instrumentation with minimal effort relegated to exploratory research and developmental efforts necessary for the generation of a basic understanding of the underlying phenomena involved. At the present time, the inability of the ultrasonic evaluation methods are seriously limiting the effectiveness of fracture mechanics to establish current design criteria.

Successful flaw detection involves two basic requirement. First, the flaw must be bathed with ultrasound and second, some ultrasound must return to the interrogating transducer. A critique of the present state-of-the-art of the ultrasonic method has shown that there is a general preoccupation for the first detection requirement. The second requirement receives very little attention. It is assumed that the surface contour and roughness

of natural flaws will provide the necessary beam divergence of the flaw radiation to facilitate detection. It has been shown that the latter is not a valid assumption to base the detection process upon. It is evident that all conventional flaw detection procedures currently in use are amplitude dependent.

The flaw characterization processes are, for the most part, taken directly from the data acquired during the detection process. Very few attempts are made to separate and optimize the detection and characterizatfon processes. Size determinations are made almost entirely by invoking the direct relationship between amplitude response and flaw area. Such determinations are only valid under very restricted conditions. One can cite limiting factors associated with the flaw, system parameters and procedures. The salient flaw characteristics are orientation, contour, and surface roughness while system parameters include transducer size, shape and frequency. Theee factors individually or collectively can render present flaw characterization techniques ineffective. It is even impossible to associate large flaws with large amplitude response. For example, an adversery oriented flaw can produce a much smaller amplitude response than a small favorably oriented flaw. There are some amplitude independent flaw characterization techniques, however it appears that such procedures have been confined to the laboratory. The literature is essentially void of instances of field age.

The detection process was modelled to investigate the inherent abilities and reliabilities for the detection and characterizaiton of planar, totally embedded flaws. The latter flaws were chosen €or study since it represents the most difficult flaw to detect and characterize. The model used is based upon the spatial interplay of the radiation fields from the transducer and flaw. Analyses indicate that the amplitude-flaw area relationship is substantially affected by material attenuation and flaw characteristics such as location and orientation. For example, if one uses a base metal DAC curve as an amplitude standard, the added weldment attenuation can account for an order of magnitude decrease or degradation in amplitude. It was found that flaw orientation or more properly, the misorientation of the flaw with respect to the interrogating beam is the greatest cause of amplitude degradation. As an illustration, a nominal size angle shear transducer (1/2" diameter) operating at 2.25 MHz would experience an amplitude degradation of 15 and 32 db while detecting a 10^{o} misoriented flaw of 1/4" and 5/8" in

diameter, respectively. The greater amplitude degradation for the larger flaw is due to the fact that its radiation field is less divergent, thus making it more difficult for alignment with the radiation field of the interrogating transducer. The amplitude advantage noted at zero misorientation is lost with increasing flaw misorientation angle. For the above transducer both the 1/4" and 5/8" diameter flaws would give the same response at a misorientation angle of 8 degrees. Beyond this point the smaller flaw would produce the greatest amplitude response. One connotation of this observation is that an adversely oriented flaw would produce less amplitude response with flaw growth. It was found that such inabilities increase with the size of the transducer.

Using the model, probability of detection (POD) plots as a function of flaw size and misorientation angle were generated. Unlike the monotonically increasing POD with flaw size for surface flaws, the POD for misoriented embedded flaw can decrease to zero once a critical size has been attained. It is also possible that certain misoriented flaws will have a POD of zero regardless of its size.

The above remarks pertaining to detecting ability and reliability were verified by extensive experimentation on simulated flaws - i.e., flat bottom holes at various misorientation with respect to the interrogating beam. It should be pointed out that the above analyses are an assessment of what one may term as the systematic contribution of the reliability of the ultrasonic detection process. As such the assessment must be looked upon as being representative of the optimum detecting ability. The random influence of the operator and variations in material or flaw characteristics such as surface roughness and contour will always detract fromthis optimum or nascent ability.

As part of this program two amplitude - independent flaw characterization techniques were evaluated by analytical and experimental means. The first makes use of the location of the maximum amplitude while the second derives intelligence from the minima of the spectral response. In both of these techniques it was found that by making two independent measurements it was possible to determine the true flaw size and orientation. These techniques show great promise from the standpoint of ease and accuracy. They will be examined in greater detail with real flaws during the second phase of this program.

In summary, the work of this report has indicated those parameters involved in the general process of flaw detection by the ultrasonic method. Analytical and experimental results indicate that the flaw misorientation

is the limiting factor to successful flaw detection and characterization. This limitation is due to the total dependence upon the amplitude of the response from a flaw. To this end, amplitude - independent flaw characterization techniques were examined. Such techniques appear to be more accurate and, what is more important, they give equal preference to both large and small amplitude response from flaws.

III. INTRODUCTION

The ever increasing demands upon existing material/design combinations have necessitated the need for greater reliability. To this end, fracture mechanics is being used to generate guides for acceptable flaw content based upon anticipated operating environments. The effectiveness of fracture mechanics is predicated upon the accurate quantitative assessment of the flaw content as typified by number, shape, size, orientation and location. Such assessments are necessary for the assurance that all unacceptable elements of the flaw content have been eliminated. The detection and characterization of a given flaw content must be performed with the methods and procedures of the nondestructive mode of evaluation. The highly quantitative nature of the flaw content assessment that is necessary has been responsible for the creation of appreciable demands upon the field of nondestructive testing. These demands have been manifested in a number of ways. During the last decade there has been an intensification in the search for new nondestructive testing methods and optimization of existing methods. Perhaps, one of the major effects of fracture mechanics upon nondestructive testing has been the realization of the need for the determination of the reliability associated with each nondestructive method.

The initial subdivision of the methods of nondestructive testing is based upon whether the flaws to be detected are surface or subsurface. The surface flaw is one that is near or breaks through the surface. A subsurface flaw is totally embedded and is free from any effects that may be produced by the confines of the material/structure being interrogated. The detection and characterization of surface flaws has been the subject of a number of impressive studies.[1-4] These studies have included the determination of the reliabilities of the major nondestructive testing methods. The results will be summarized in appropriate sections of this report. The quantitative definition and determination of the reliability of the detection and characterization of totally embedded flaws has not received any substantial attention as yet. Efforts to date have included some impressive theoretical analyses[5-7] while the experimental substantiation, for the most part, has consisted of a round

robin type of activity. The latter have often been based upon ill conceived notions and further complicated by improper data analysis. There have been some attempts to extrapolate the surface flaw situation to that of totally embedded flaws.[8] One must appreciate the fact that the methodology available for the detection and characterization of surface flaws are unique to the particular flaw content involved and cannot be directly applied to the case of the totally embedded flaws.[9] One must be careful in generalizing the abilities and reliabilities of surface flaw detection to the total spectrum of the flaw content. The physical principles involved in detection and characterization must be examined to note applicability.

As the location of the flaw generated a natural division of the nondestructive methods, the nature of the flaw (globular vs. planar) can also subdivide the applicable methods. Planar flaws such as cracks are much more difficult to detect. Therefore, this program is primarily concerned with those methods that can quantitatively characterize totally embedded planar flaws.

For the detection of volumetric or subsurface flaws two nondestructive evaluation methods are used -- i.e., radiography and ultrasonics. The use of radiography is limited to flaws that have an appreciable thickness in the direction of the penetrating radiation.[10,11] Both the radiographic and ultrasonic methods are affected by the orientation of the flaw with respect to the interrogating radiation beam.[12,13] However, the susceptibility of ultrasonics to orientation effects is considerably less. Moreover, the ultrasonic method is capable of detecting flaws that have thickness in the realm of angstrom units for the case of a crack and within mils for the common inclusions of most metals.[14] The latter is for interrogations at nominal frequencies of 1 to 5 MHz. It should be pointed out that the radiographic and ultrasonic methods are not totally complementary. There are a number of instances where a given flaw content would be undetectable by both methods. There is a good deal of documentation of the comparative abilities of the two methods.[15-17]

When one considers the detection of weldment flaws a number of diverse complications become apparent and must be taken into consideration for

meaningful quantitative flaw characterization. The weldment invariably has high attenuation and is anisotropic in both velocity and attenuation.[18,19] The weld structure is often composed of large diameter elongated dendritic grains. Such a structure can produce erroneous flaw locations for bonified flaws and can generate false flaw indications. *The* geometry of the weldment in conjunction with base materials and back-up plates is also responsible for artificial reflectors and false flaw indications.

The almost total dependency upon amplitude data is responsible for generating the inadequacies of the present day ultrasonic weld interrogation techniques and procedures. To this end, there has been a significant amount of research pertaining to imaging techniques. It would appear that the potentials of flaw imaging by appropriate processing of conventional A, B, C and P-scan data are being unjustifiably overlooked for the more new and exotic techniques as typified by holography.[20,50] The report will assume that the reader is acquainted to some measure with the general field of nondestructive testing but is not necessarily an expert in the ultrasonic evaluation of weldments.

IV. LITERATURE SEARCH

The literature search on ultrasonic weld interrogation examined a number of sources. One source was the open literature. The initial search of the open literature was performed by computer retrieval services as provided by the Lockheed/DIALOG system. Descriptor words such as ultrasonic, weld, inspect and their various forms were used. The COMPENDEX file for COMPuterized ENgineering inDEX yielded 198 finds while the WELDASEARCH file produced 132 finds. A printout of each find was obtained which listed identifying particulars and a copy of the author's abstract. Based upon a review of the abstracts copies of the more informative papers were ordered for closer study and evaluation.

Another phase of the open literature search consisted of scanning the journals and conference reports of societies with a specific interest in the evaluation of weldments. Copies of all germane papers were obtained for more careful scrutiny and cataloging. Table I lists these journals and their respective review periods. In addition, government, industrial and professional society procedures and specifications were sought. The results in this category were minimal. Proprietary measures prevented the listing of procedures and specifications of the private industrial sector. However, it is felt that all such information is contained within the assembled documents of the topical index. A quite fruitful source of information were the discussions with people of known expertise and interest in weld interrogation and evaluation.

A total of 213 papers and documents were assembled as a topical index; see Table 11. The compilation of such information is representative of the present state-of-the-art of weld interrogation. Abstracts of each paper or document are listed by an identifying number corresponding to its tabulation in the Appendix. It is not the intent of this index to list all the available papers within each category. A selection process was initiated to limit the papers to those that are representative and can contribute to the index. In the event that it was observed that the author's abstract for a critical paper is not complete, a revised abstract is given and so indicated.

The categories of the topical index were selected to encompass the subject matter as well as general background material on the ultrasonic interrogation method. An attempt has been made to include both theoretical and experimental investigations. Moreover, the categorization of the topical index presents a datum plane of reference for all levels of expertise.

TABLE I

JOURNAL SEARCHED

AMERICAN WELDING SOCIETY JOURNAL (1937 - Present)

BRITISH JOURNAL OF NON-DESTRUCTIVE TESTING (1961 - Present)

BRITISH WELDING JOURNAL (1954-1968)

Metal Construction and British Welding Journal (1969-1974)
Metal Construction (1975 - Present)

DEFEKTOSKOPIYA (Soviet Journal of Nondestructive Testing) (1965 - Present)

INSTITUTE OF ELECTRICAL & ELECTRONICS ENGINEERS (1970 - Present)

(TRANSACTIONS ON SONICS & ULTRASONICS)

INTERNATIONAL JOURNAL OF NONDESTRUCTIVE TESTING (1971 - Present)

MATERIALS EVALUATION (1953 - Present)

ULTRASONICS (1963 - Present)

TABLE II

TOPICAL INDEX

ULTRASONIC WELD INTERROGATION/EVALUATION

*Indicates paper numbers and listing in the Appendix

VIII FACTOR INFLUENCING FLAW DETECTION AND CHARACTERIZATION

1. Cladding (78, 84, 90, 108, 109)
2. Materials
   a) Pearlitic (19, 110)
   b) Stainless Steel (35, 99, 110-120)
   c) Inconel (121)
3. Weld Configuration (121-123)
4. Artificial Reflections (36, 95, 111, 115, 122-125)
5. Attenuation (35, 99, 110, 112, 117-119, 121, 126, 127)
6. Course Grain Structure (35, 99, 110, 114, 115, 118, 128, 129)
7. Microstructure (35, 99, 114-117, 128, 130, 202)
8. Noise (99, 115, 117, 118, 126, 128, 131)
9. Shear Wave Polarization (110, 114, 121)
10. Operator (36, 59, 108, 132-134)
11. Pressure (135, 136)
12. Flaw Orientation (75, 78, 101, 139, 140, 141-144)
13. Flaw Surface Roughness (75, 137, 138)
14. Interrogation Surface Roughness (145-147;

IX RELIABILITIES (1, 91, 139, 144, 148-151)

X NEW/NOVEL FLAW CHARACTERIZATION TECHNIQUES

1. Spectroscopy (152-157)
2. Radiation Variations (158)
3. Location of Maximum Amplitude (92)

XI FLAW DETECTION MODELS (91, 101, 139, 140, 144, 159, 160)

XII GENERAL BACKGROUND INFORMATION

1. Transducers
   a) Radiation fields (162-167)
   b) Focusing Action (168-172)
   c) Arrays (173-176)
   d) Evaluation (177-180)
2. Reflection from Various Shaped Reflectors (67, 181-184)

V. THE STATE-OF-THE-ART OF ULTRASONIC METHODS

Prior to any discussion of the procedures and techniques of the ultrasonic weld interrogation method, it would be advantageous to acquaint the reader with the general concepts involved in the interrogation of homogenious materials. This will provide the understanding necessary to appreciate the subsequent discussions involving inherent abilities and limitations of the available techniques and procedures involved. Moreover, such work will provide the basis for suggesting improvements for flaw detection and characterization.

It is important that one realize the difference between the flaw detection and characterization processes. As the phrase flaw detection implies it is the process where an anomaly is noted and located either with respect to the interrogating transsucer(s) or with respect to a specimen coordinate system. The detection event, including location data, is a prerequisite for flaw characterization. Flaw characterization, as used in this report, involves a minimum of interrogation and is the associated measurements and deduction process which discerns the characteristics of the flaw -- e.g., size, location, orientation and shape.

1. Flaw Detection Process

All the procedures of the ultrasonic flaw detection have one common factor -- i.e., they are all amplitude dependent. Successful flaw detection by the pulse-echo procedure is based upon two necessary conditions. First, some ultrasound must strike the flaw and, second, some ultrasound must reach the interrogating transducer. This is illustrated in Figure 1 for the case of the straight or normal beam interrogation. The radiation fields from both the transducer and flaw or reflector are shown and detection is essentially governed by the spatial interplay of the two fields. The amplitude response at two positions of the traverse of the transducer on the interrogation surface are shown. At position A, a substantial amount of ultrasound strikes the reflector as indicated by the radiation field in the direction of the reflector. However, because of the relative orientation of the reflector with respect to the beam, essentially none of this ultrasound returns to the interrogating transducer. At point B much less ultrasound impinges upon the reflector, but because of the favorable alignment of the radiation fields involved, an appreciable amount of ultrasound returns to the transducer. The overall effect,

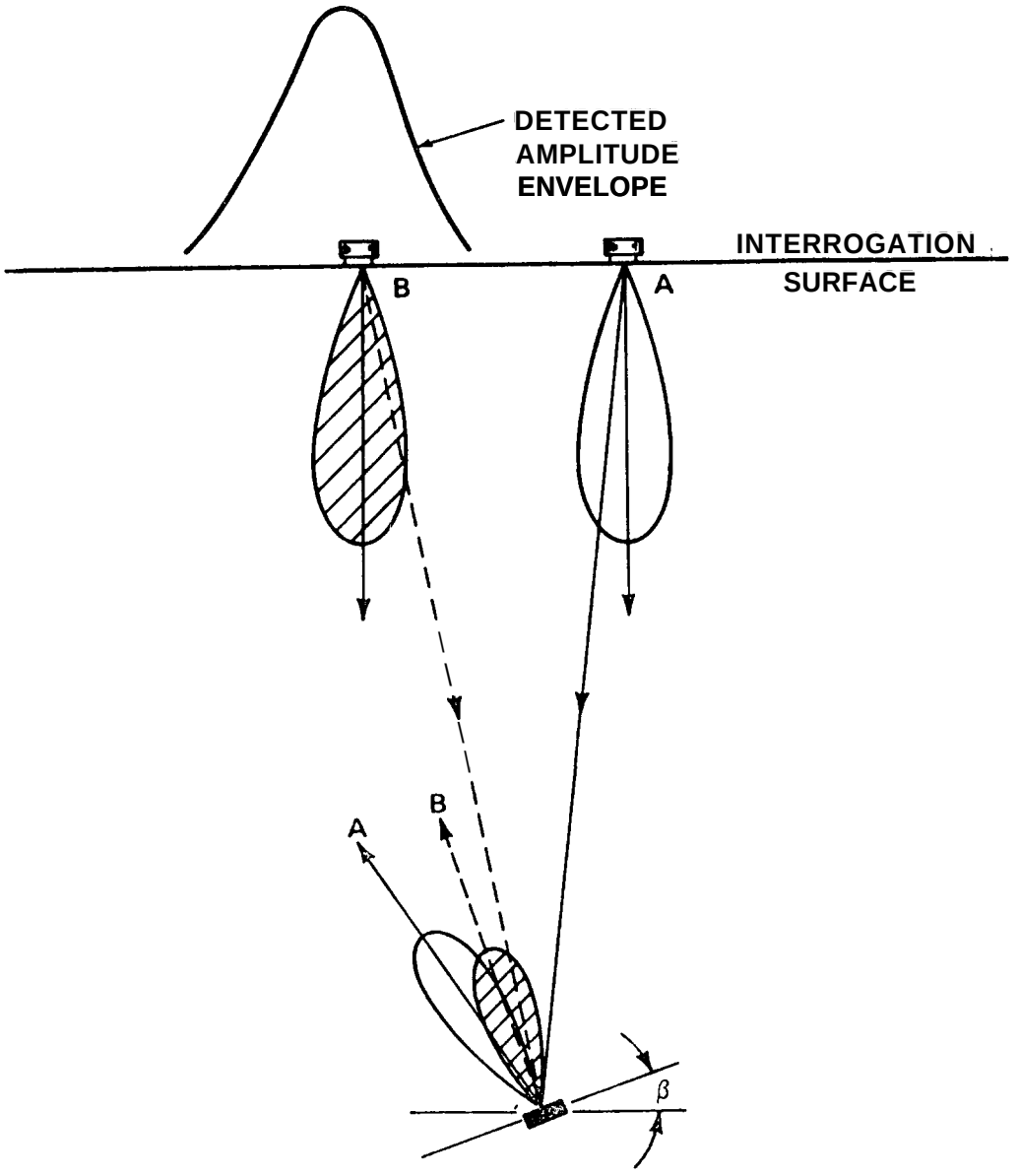

Figure 1 - The pulse-echo flaw detection process in terms of the spatial interaction of the radiation fields of both the transducer and flaw. After Serabian and Lawrie (21).

as one performs a transverse scan, is that the amplitude first increases, maximizes, then decreases to produce essentially a bell shaped amplitude display. Much the same considerations apply for an interrogation by an angle beam. The form of interrogation shown in Figure 1 is the most widely used process and will henceforth be referred to as the conventional flaw detection process.

a. Theoretical Analysis

The above described detection process as described in Figure 1 is one form of echodynamics; a term used by Gurvich[7] to characterize the locus of the amplitudes observed in terms of transducer motion. In Figure 1, the transducer motion involved is directly over the flaw. Gurvich shows a number of other possible forms of echodynamics; see Figure 2. A number of models have been generated for the amplitude response envelope shown in Figure 1.[5,6] A more recent model[21] involves a great deal of generalization and will be used to indicate the factors that influence the detected amplitude response.

Figure 3 indicates the geometric parameters of the model for the straight and angle beam interrogations. It will be assumed that the distances between the reflectors and transducer are such that the far field of radiation is involved. This is a reasonable assumption since most interrogations are performed within the far field. It will also be assumed that the reflectors are flat and smooth and also that both reflectors and transducers are circular. The latter requirement is not a necessity; however, it does greatly simplify the experimental verification of the model. The amplitude response $A(\theta)$ is given in terms of the sampling parameter (θ). In this manner all specifics of reflector distance and specimen geometry are obviated. In each case of Figure 3, the relative magnitudes of ultrasound from the transducer and reflector are determined by the radiation directivity function evaluated at θ_T and θ_R, respectively. Also, for the sake of generalization, the reflector and transducer sizes will be considered in terms of the predominant wave length involved: $n\lambda$ and NA for the reflector and transducer diameters, respectively. With such notation the directivity function, for example, for a circular transducer is only a function of N and is given by

$$D_T(\theta) = \frac{2\,J_1\,(\pi N \sin\theta)}{\pi N \sin\theta} \qquad (1)$$

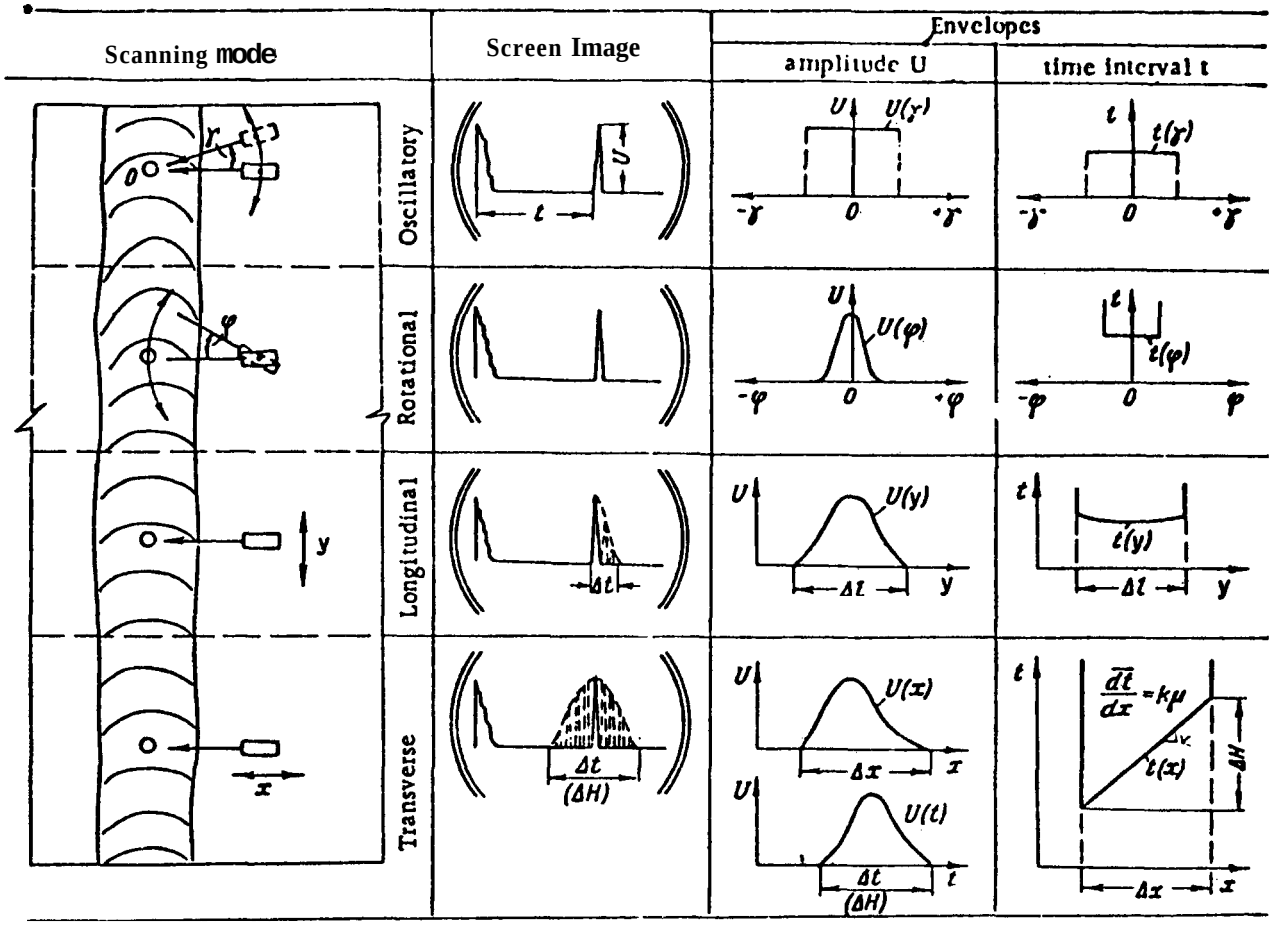

Figure 2 - Amplitude and time envelopes of various forms of weld interrogation echodynamics. After Gurvich (7).

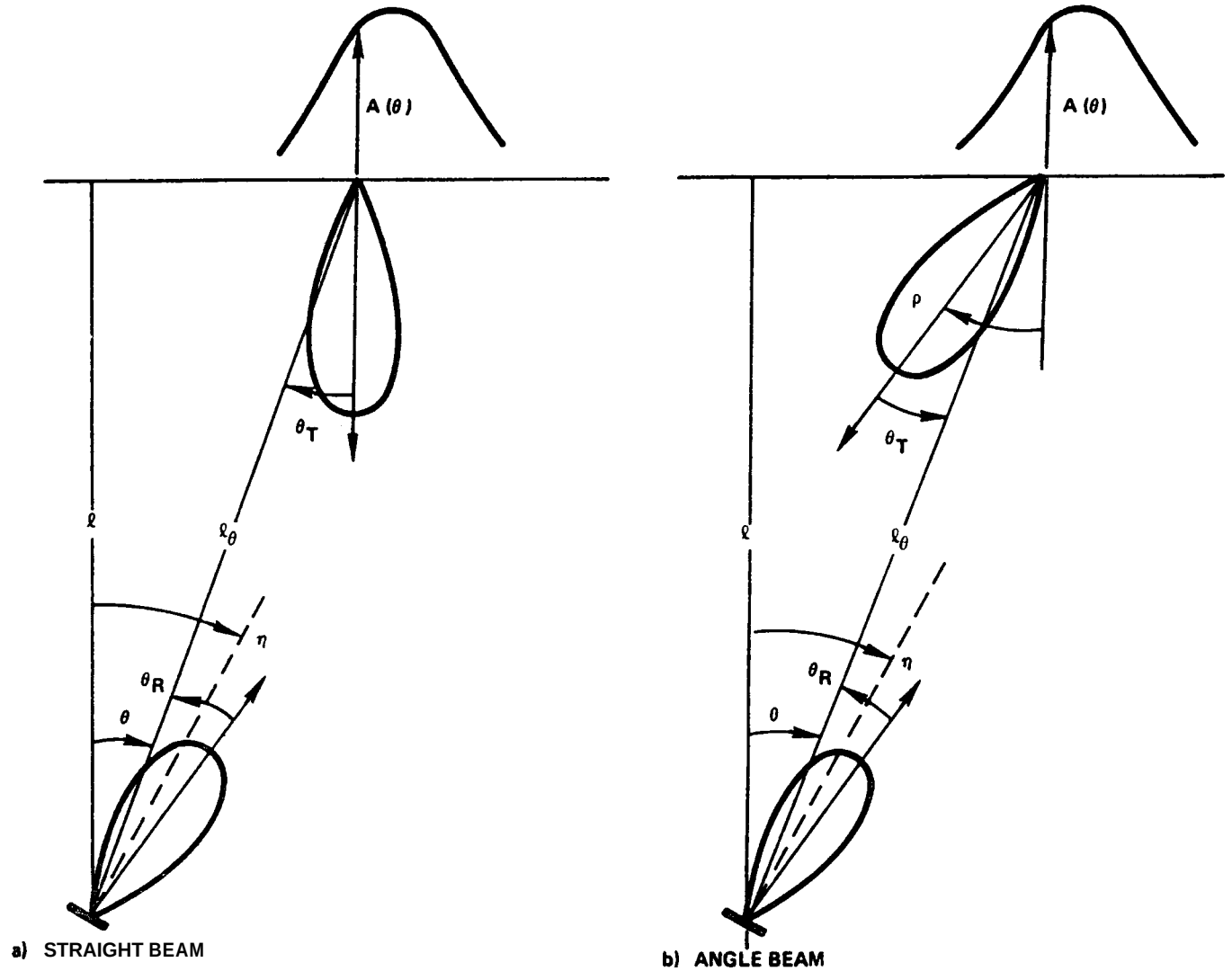

Figure 3 - The salient model parameters and their associated symbols for interrogation from a flat surface. After Serabian and Lawrie (21).

where J_1 is the first order Bessel function of the first kind. It should be mentioned that radiation outside the main beam will be neglected. Although the derivation of such directivity functions involves continuous waves there is ample evidence that indicates their use for pulsed ultrasound.[22]

It is imperative that the orientation of the reflector is defined in a meaningful manner. It is much more advantageous to speak of the misorientation (ϕ) with respect to the interrogating beam, as in Figure 4. Thus, the misorientation angles are η and $\eta-\rho$ for the straight and angle beam interrogations, respectively. The angle η is the inclination of the plane of the reflector while ρ is the entry angle of the angle beam. This means that the amplitude response is only dependent upon the misorientation angle with all other factors being equal.

If we calibrate the amplitude response in terms of a reflector size of $n_\theta\lambda$ oriented perpendicularly to the interrogating beam, the model yields the amplitude response for a reflector of $n\lambda$:

$$A(\theta) = \underbrace{\left(\frac{n}{n_o}\right)^2}_{F_1} \underbrace{D_T^2(\theta_T)D_R(\theta_R)\cos\frac{\theta_R}{2}}_{F_2} \underbrace{\left(\frac{\ell o}{\ell_\theta}\right)^2 e^{-2(\alpha\ell_\theta-\alpha_o\ell_o)}}_{F_3} \qquad (2)$$

where D_T and D_R are the radiation directivity functions of the transducer and reflector, respectively. The constant α is the attenuation and ℓ is the reflector distance involved. The subscripts on α and ℓ provide for calibration in an external standard with its own attenuation (α_o) and flaw distance (ℓ_o).

As indicated in Equation 2, the amplitude response is composed of three functions which are diagrammatically shown in Figure 5. The first function, F_1, indicates that the amplitude response is proportional to the area of the reflector. This is a desirable relationship and facilitates true reflector size determinations taken directly from the amplitude response. The second function, F_2, indicates the amplitude loss or degradation due to any misorientation between the reflector and the interrogating beam. It is significant to note that the amount of amplitude degradation increases with either an increase in the reflector size (n) or the transducer size (N). Moreover, it should be noted that for any combination of reflector and transducer sizes there is a

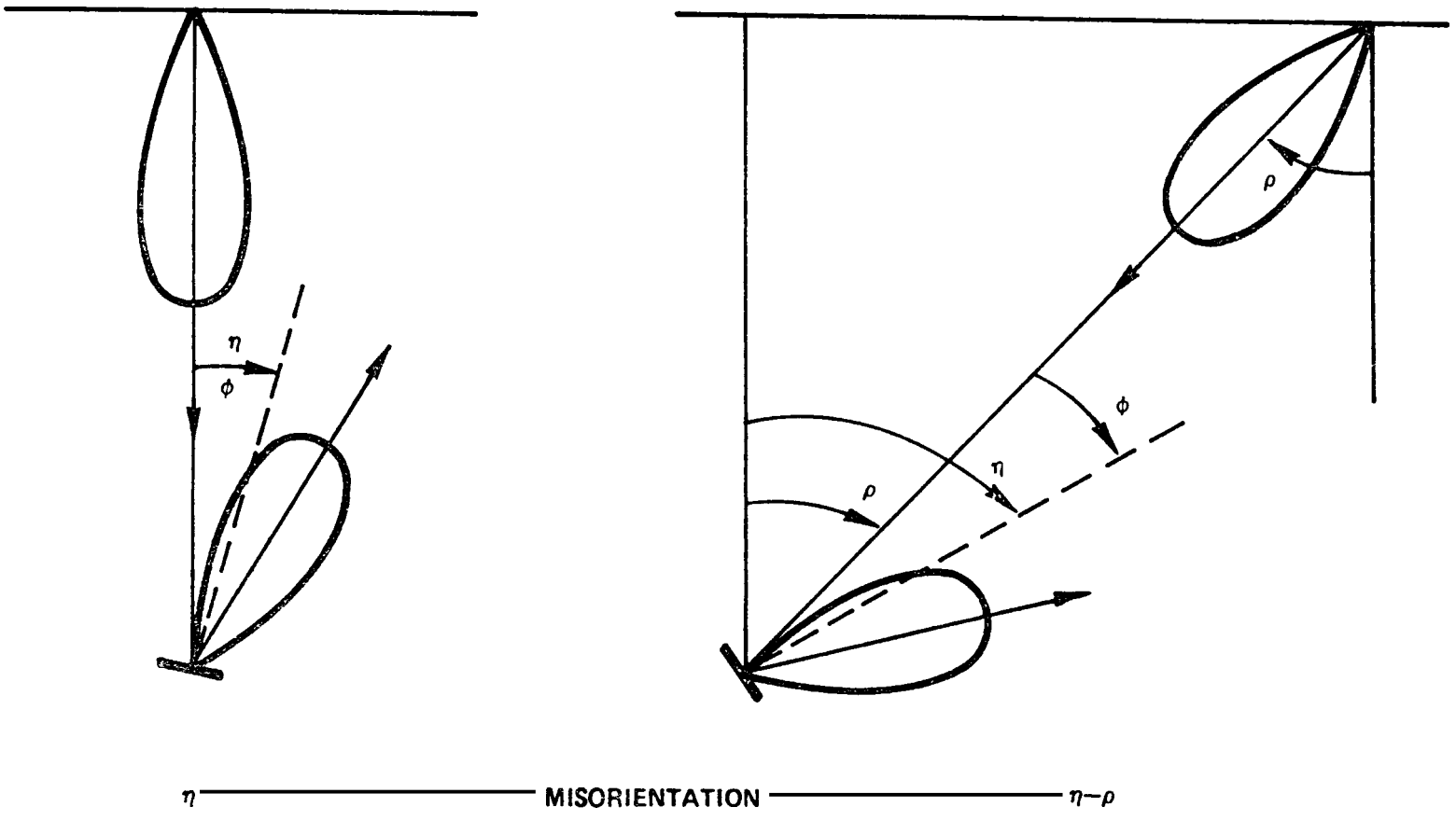

Figure 4 - The flaw orientation angle (4) for straight and angle beam interrogations. After Serabian and Lawrie (21).

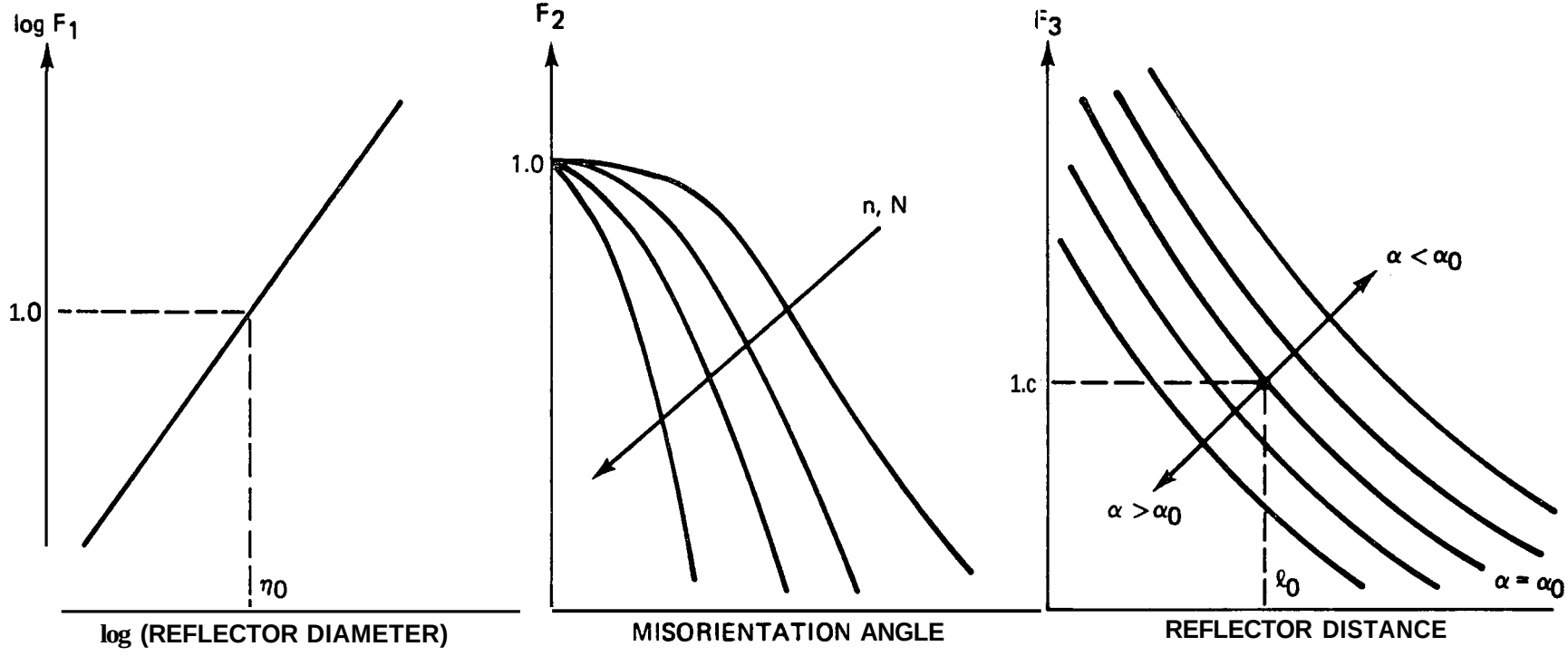

Figure 5 - Diagrammatical representation of the three functions responsible for the amplitude response envelope of the model.

reflector misorientation where detection is essentially not possible. The third function contains the influence of material attenuation and the location of the reference reflector. The effects of this function can be appreciably minimized or eliminated by proper calibration procedures. Therefore, the amplitude degradation due to reflector misorientation is the flaw characteristic which has the most influence on the observed amplitude response.

Figure 6 displays the computer runs of the amplitude envelopes or scan signatures for a scanning transducer whose diameter is 3 wavelengths (N=3) for a variety of reflector sizes (n) with a misorientation angle of 10 degrees from the beam. It is assumed that the function F_3 of Equation 2 is unity, - i.e., that its variation is negligible. The use of transducer and reflector size normalization by the wavelength renders such displays applicable to any frequency and type of ultrasonic wave. Moreover, the generalized notation allows one to view this data as representing the results of a straight beam interrogation of a reflector whose normal is inclined ten degrees from the vertical. Likewise, the data may be looked upon as representing an angle beam interrogation of a reflector whose normal is inclined 70 degrees while using an entry angle of 60 degrees, a reflector inclination of 55 degrees for a 45 degree entry angle, or in general, a reflector inclination of $\rho \pm \phi$. As the reflector size is increased three distinct characteristic changes occur in the amplitude response envelopes typified by Figure 6. It can be seen that the detected amplitude increases (see normalization gain), there is a decrease in the lateral extent of the envelopes and the location of the maximum amplitude on the interrogating surface approaches the misorientation angle. All intelligence from the conventional ultrasonic interrogation methods is derived from one or more of the latter three amplitude response envelope characteristics.

As previously indicated, the misorientation angle is most responsible for amplitude degradation. This is indicated in Figure 7 for the case of a misorientation angle of 5°. It can be noted that for a small transducer $N \leq 2$) the amplitude-reflector size relationship is linear and is essentially the function F_1 of Figure 5. The amplitude has been calibrated with the response from a reflector whose diameter is 2λ or $n_o = 2$ of Equation 2. This is an arbitrary standard, however, its selection does not interfere with the observation of amplitude differences. It is apparent that for transducer size of $N \leq 2$ the beam diameter is so wide spread that a transducer

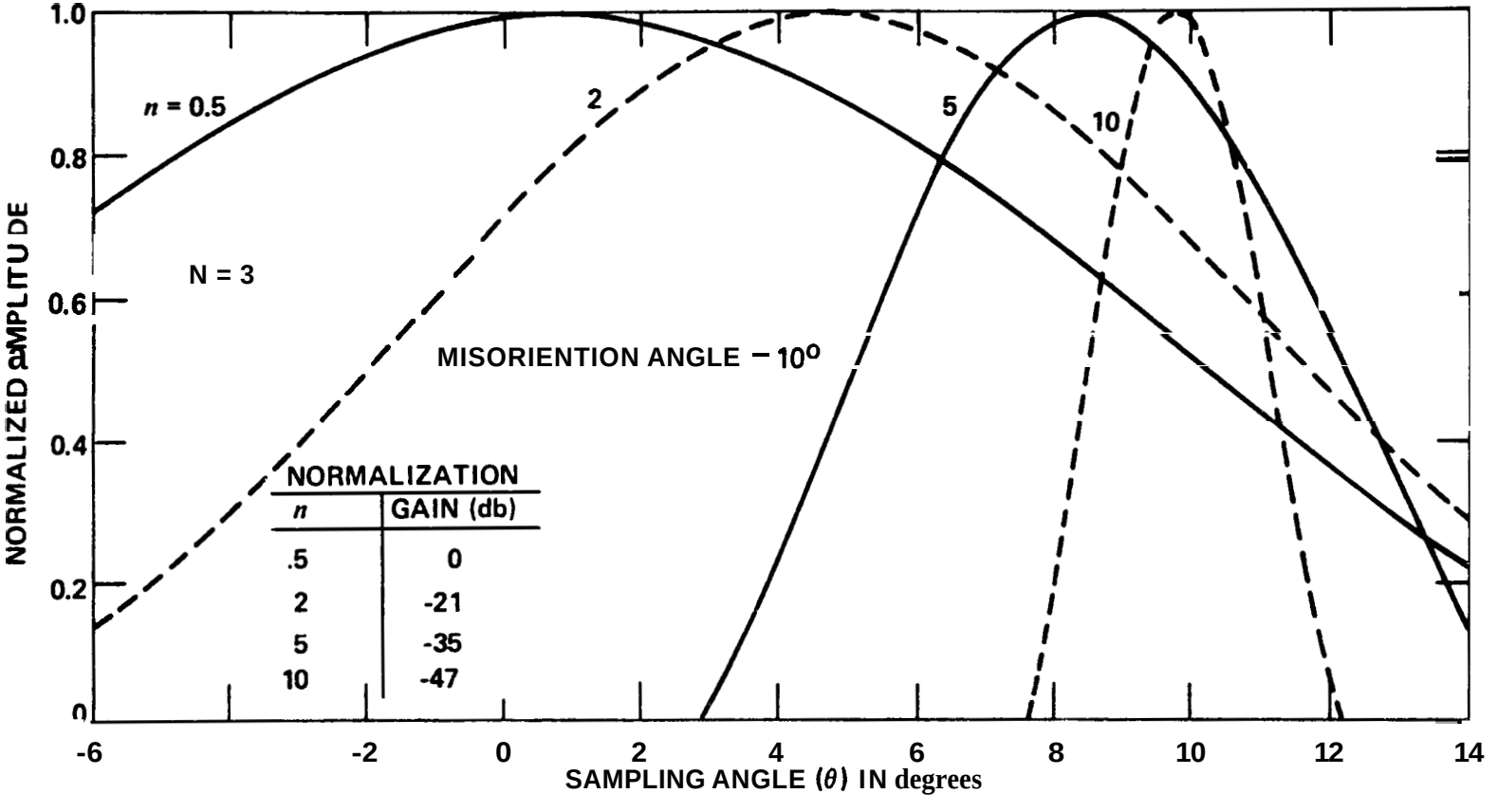

Figure 6 - Amplitude response envelopes or scan signatures for a variety of reflector sizes as noted by a transducer whose diameter is three wavelengths; flaw misorientation angle is ten degrees. The designations n and N are the diameters in wavelength of the reflector and transducer, respectively, After Serabian and Lawrie (21).

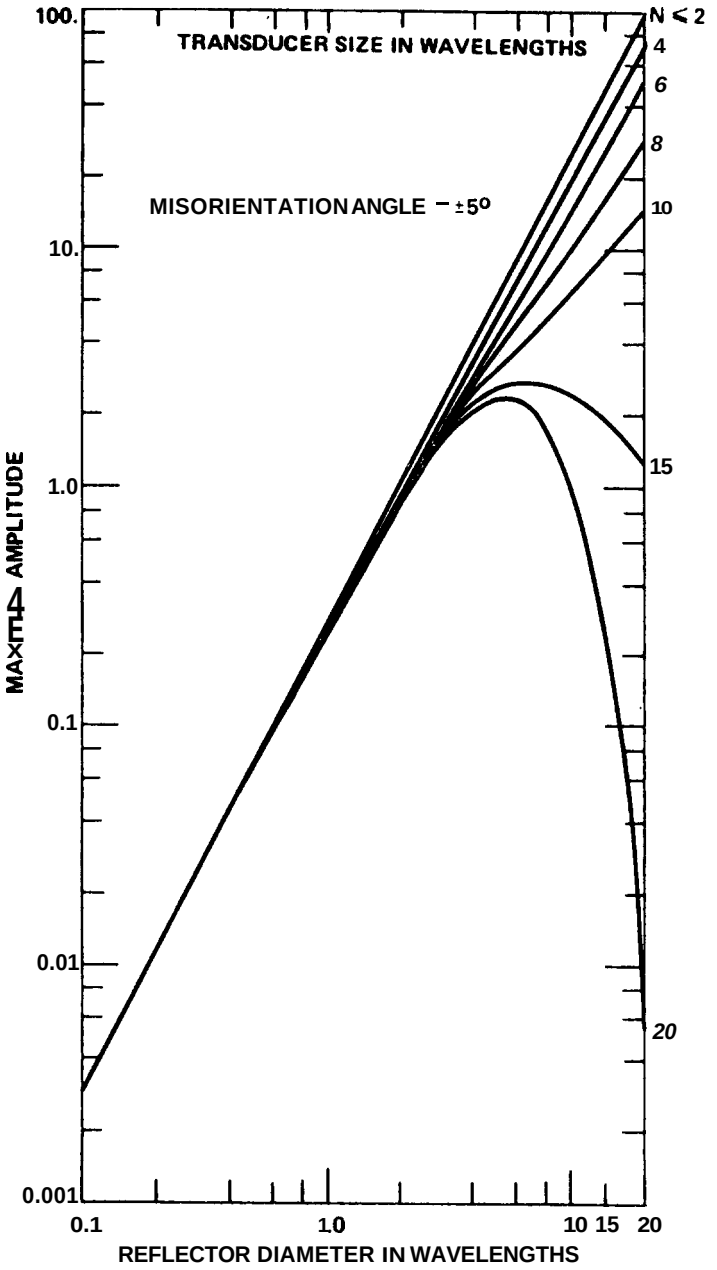

Figure 7 - Detectable maximum amplitude as a function of transducer and reflector sizes; flaw misorientation angle is five degrees. After Serabian and Lawrie (21).

position can be found to facilitate the return of the maximum possible reflection from the reflector. In effect, for sufficiently small transducers, the flaw misorientation angle has no influence upon the detected maximum amplitude. However, the real significance of the $N \leq 2$ line is that it can be used as a standard to note amplitude degradation caused by radiation field effects. It can be observed that as the transducer or reflector sizes increase the resulting radiation fields become more directional, thus reducing the ability to align the radiation fields during interrogation, and thereby, causing amplitude degradation. The amplitude degradation for any given combination of transducer and reflector would increase with misorientation angle; compare Figures 7 and **8** for the **5°** and 15° misorientation angles, respectively. The degradation in amplitude may be *so* extensive as to prohibit detection i.e., detection would involve radiation outside the main beam from the transducer and/or reflector. Such situations are indicated as solid circular terminal points in Figure **8.**

The influence of the misorientation angle upon amplitude degradation for a transducer whose diameter is 5 wavelengths is shown in Figure 9. **As** a matter of interest, the transducer sizes at the frequencies most used in longitudinal wave flaw detection in steel for the N=5 condition is also shown; all these transducers have equivalent radiation fields. The reflector sizes at these frequencies are also indicated. It can be seen that for a misorientation of 15 degrees, the amplitude from a 1/4" and 1/2" diameter flaws as noted by **a** 9/16" diameter transducer operating at 2-1/4 MHz would experience a degradation of **13** and 23db, respectively. At a 20 degree misorientation angle the dsgradation in amplitude would be **23** db for the 1/4" flaw and **58** db for the 1/2" flaw. For example, the reflector generated by a lack of fusion area on an 80° weldment face as detected by a *60* degree entry angle represents such a 20° misorientation angle situation. If one accepts 10% of the calibration amplitude as the level below which indications are not investigated, three of the four above indications would not be recorded.

The above model does not take into consideration the surface roughness of the reflector. Haines and Langston [6] have modelled this effect and

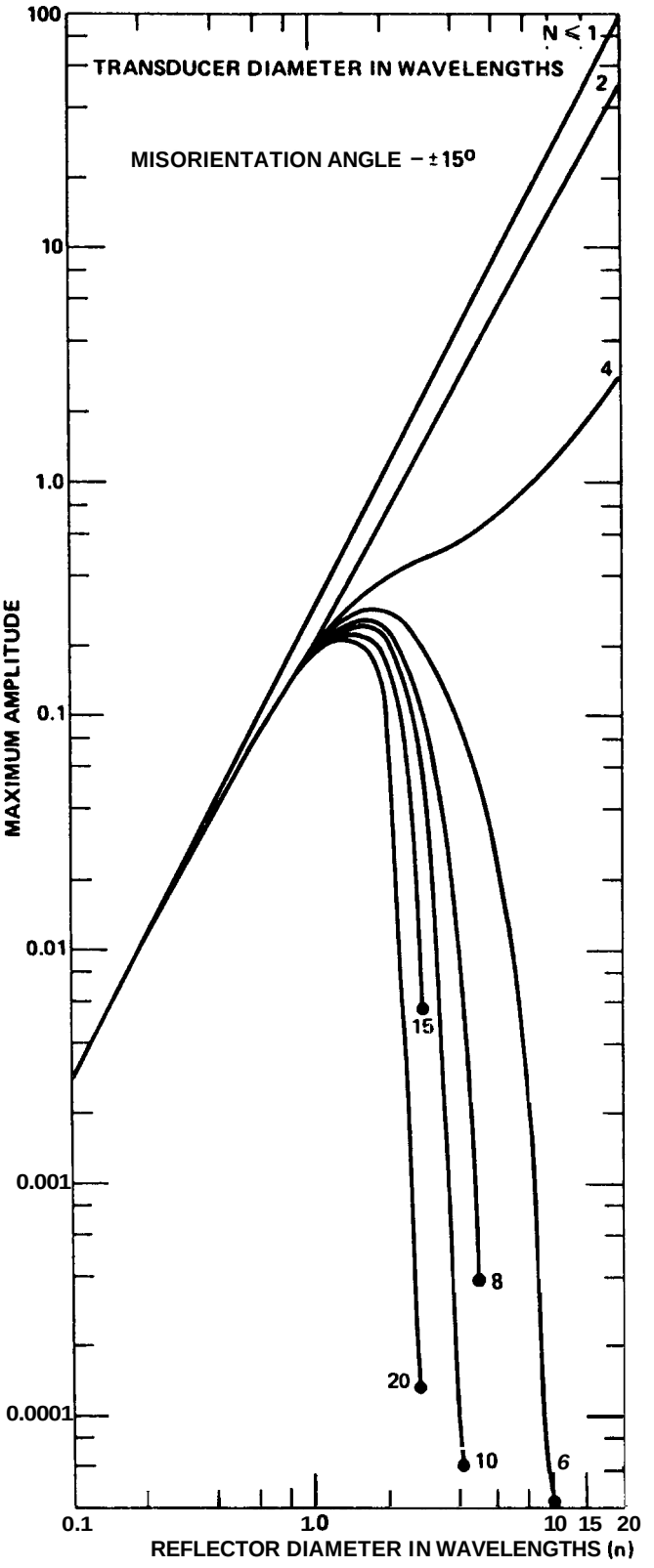

Figure 8 - Detectable maximum amplitude as a function of transducer and reflector sizes; flaw misorientation angle is fifteen degrees. After Serabian and Lawrie (21).

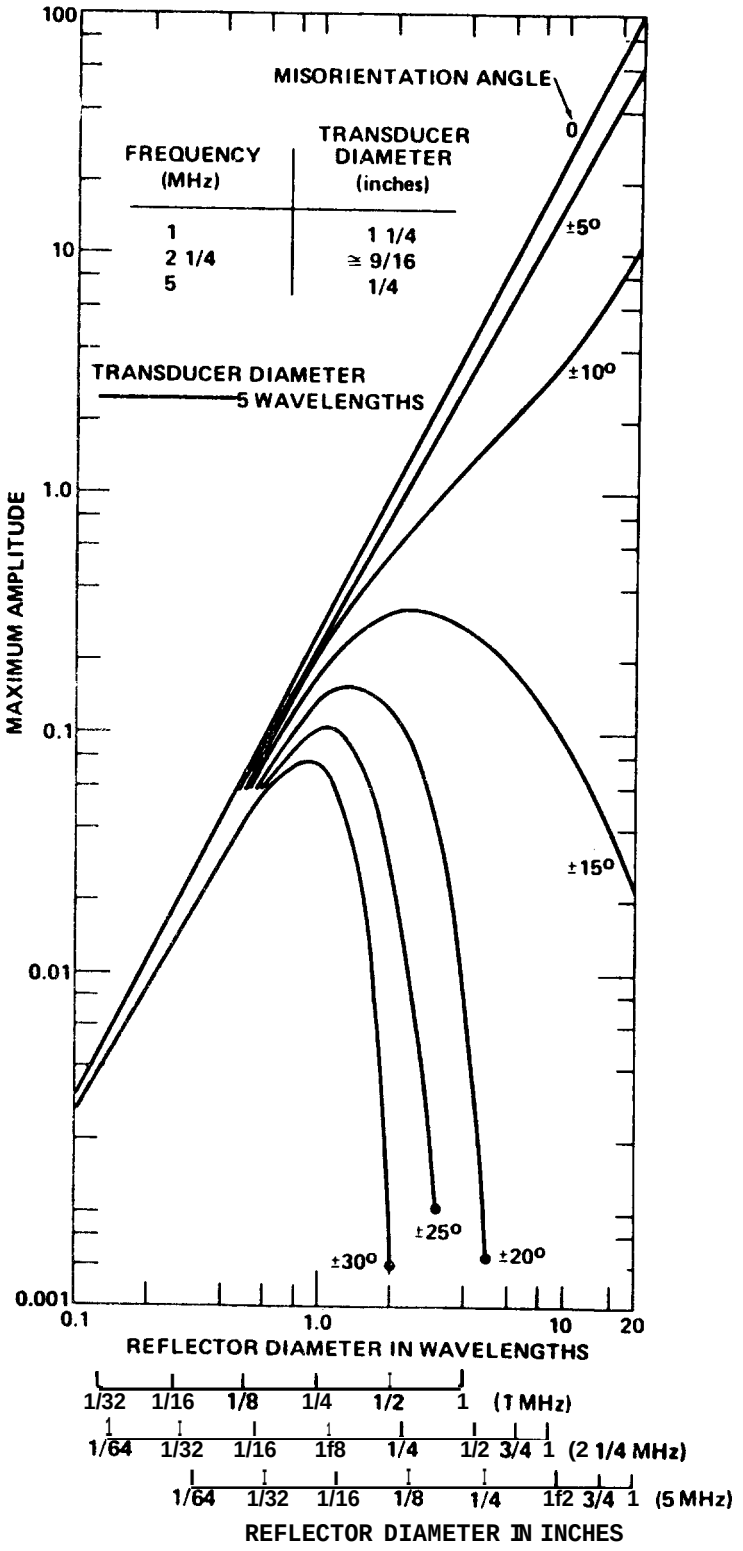

Figure 9 - Detectable maximum amplitude as function of reflector size and misorientation angle. The transducer diameter is five wavelengths. The reflector size particulars are given for the frequencies of 1, 2 1/4 and 5 MHz. After Serabian and Lawrie (21).

have found that the rough surface response is the response from an identically shaped and oriented smooth surface multiplied by a frequency dependent roughness factor. The roughness factor is independent of surface shape and size and is solely a function the ratio of the component of roughness in the incidence direction to the wavelength involved.

b. Experimental Evidence

Aluminum blocks typified by Figure 10 were used for confirmation of the model of Equation 2. [23] Flaws were simulated by the reflecting end surface of the flat bottom holes. The orientations of such reflectors were selected to provide misorientations from zero to 20 degrees with respect to a straight beam. Four different size reflectors were considered: 1/4", 3/8", 5/8" and 3/4". A total of four blocks, each with a given size reflector, were used. Figure 11 shows typical experimental data along with the appropriate amplitude response envelopes of the model.

The degradation of amplitude with the misorientation angle is shown in Figure 12. The detected maximum amplitude is very sensitive to the reflector size as well as the misorientation angle. For example, the amplitude from a 1/4" reflector experiences a 20 db reduction when the misorientation angle is increased from zero to 20 degrees. For this same range of misorientation angle the 5/8" reflector encounters a reduction of approximately 50 db. Also, note that when no misorientation exists the detected amplitude is proportional to the area of the reflector; a 16 db range for the indicated spectrum of reflector sizes. However, as the misorientation angle is increased, the amplitudes from the larger reflectors decrease much more drastically than the smaller reflectors. At a misorientation angle of 15° the amplitude advantage due to reflector area is counterbalanced by the effects of the misaligned radiation fields such that all reflectors give approximately equal response. At a misorientation of 20° the size advantage is completely lost such that the smaller reflectors produce a larger amplitude response.

Figure 13 shows the influence of transducer size and substantiates the fact that smaller transducers with their broad angular radiation fields provide better detection of the more adversely oriented flaws.

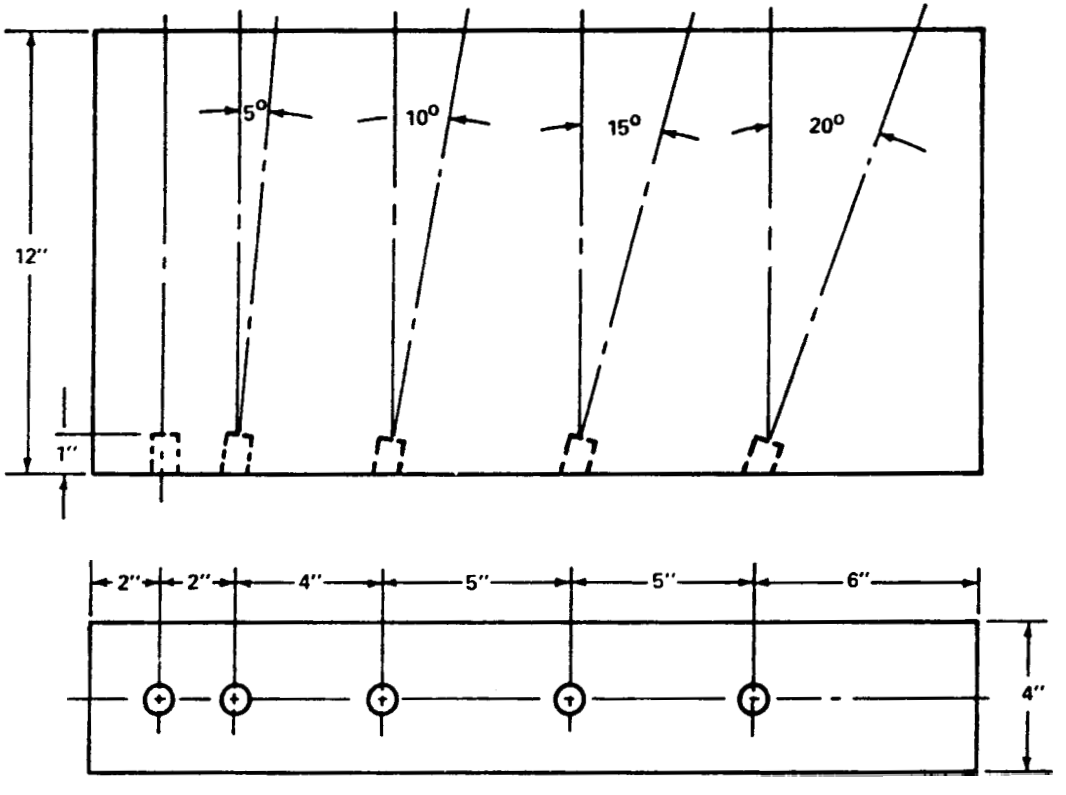

Figure 10 - The specimen used to experimentally study amplitude response envelopes. After Serabian and Lawrie (23).

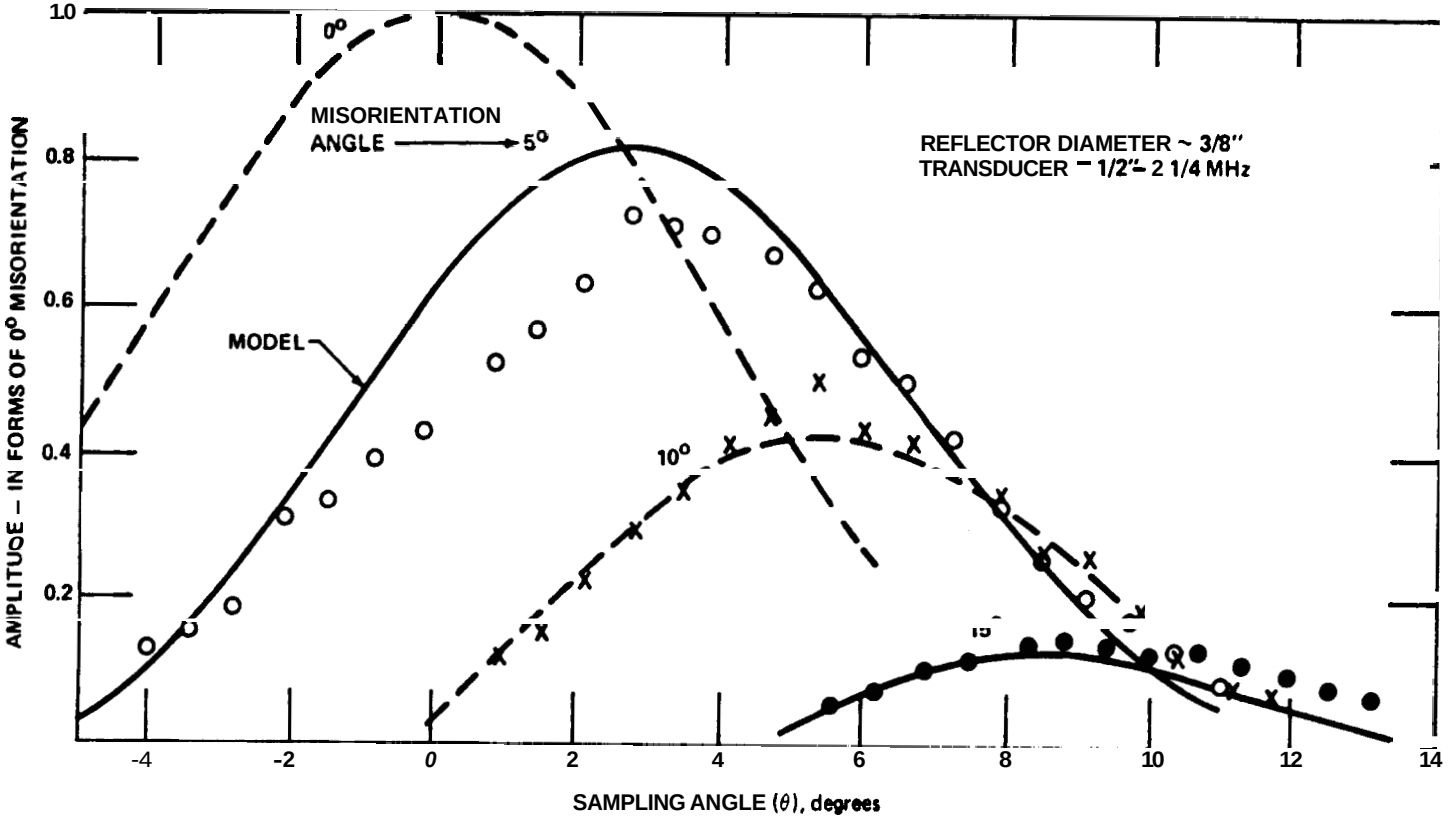

Figure 11 - A comparison of experimental and theoretical results for a variety of reflector misorientation angles. Amplitude normalization is in terms of maximum amplitude for the zero misorientation case. After Serabian and Lawrie (23).

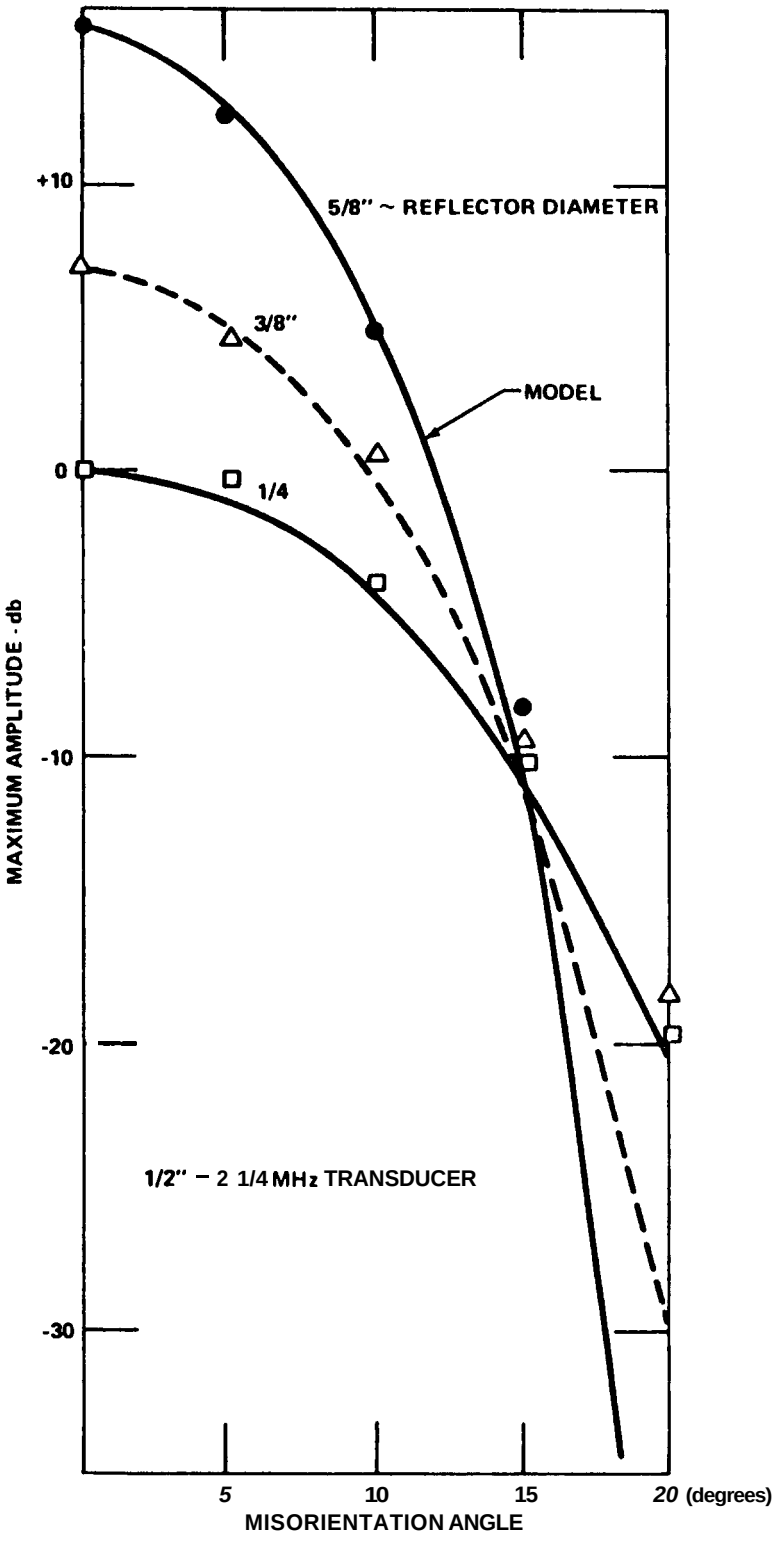

Figure 12 - Amplitude degradation due to reflector misorientatioa and size. After Serabian and Lawrie (23).

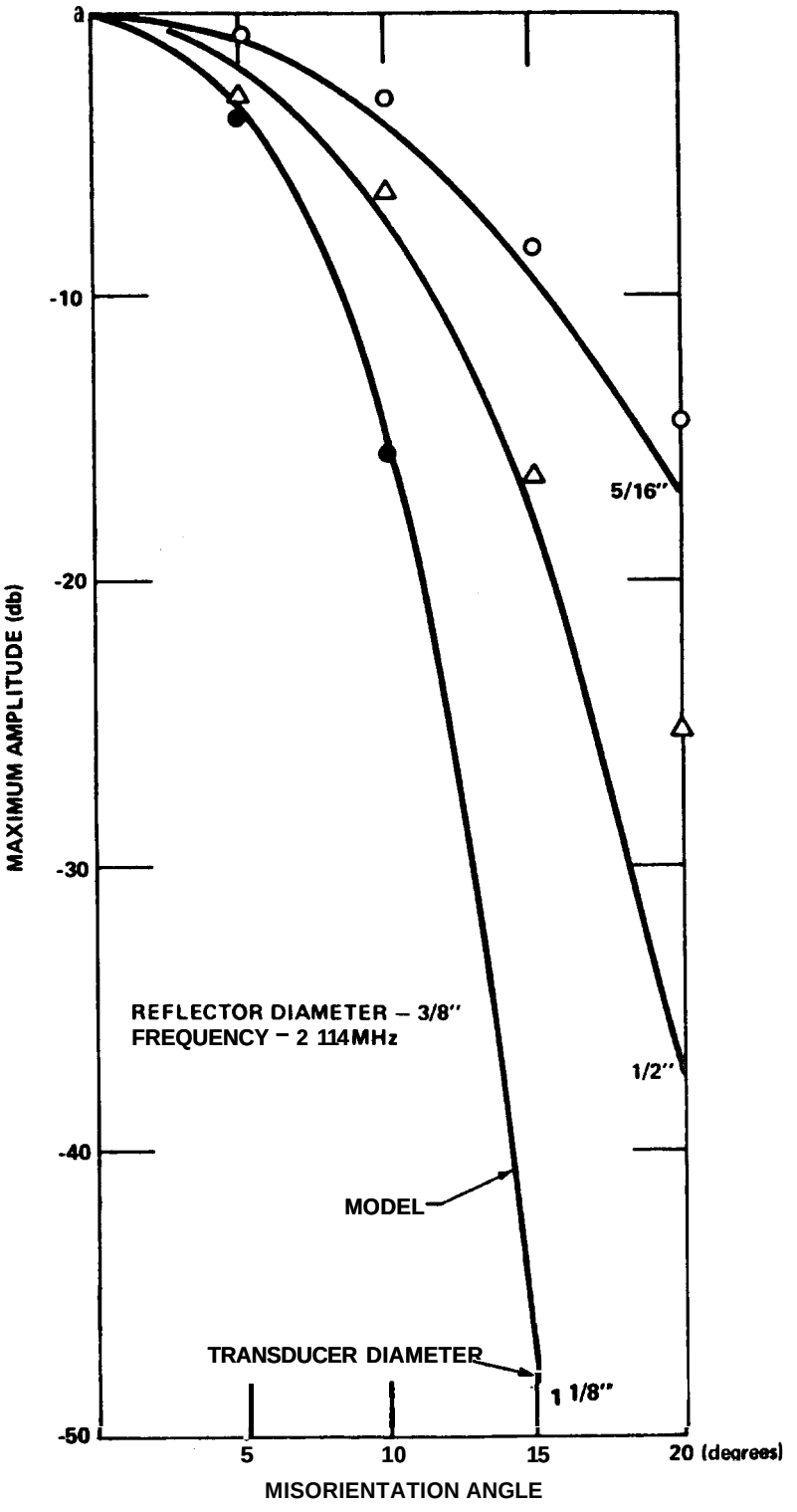

Figure 13 - Amplitude degradation due to reflector misorientation and transducer size. After Serabian and Lawrie (23).

2. Flaw zati

It must be emphasized that full flaw characterization involves the determination of size, orientation, location and shape. Location determinations involves straightforward techniques and can be accomplished quite accurately. Analysis of the error is typified by Gurvich[24] while techniques to minimize this error are given by Krug[25] and Gurvich and Desynatik.[26] Shape is perhaps the most difficult flaw, characteristic to determine. Qualitative inferences are usually responsible for such determinations.[27] For example, a wide amplitude response envelope is usually accepted as emanating from a sphere or from a cylinder when the radiation is incident upon its longitudinal axis. On the other hand, amplitude response envelopes that are narrow in extent are usually associated with planar type flaws. Also, the existence of planar type flaws may also be justified by noting an appreciable amplitude increase when two transducers in the transmitter-receiver mode are used. Such a procedure is only valid if an appropriate relative position between the transmitter and receiver can be found such that the amplitude can be maximized. Flaw size and orientation continue to constitute the major flaw characteristics that must be determined.

In the following are listed the major methods of flaw characterization as indicated by the literature search. No attempt has been male to list them in any order to indicate usage or effectiveness.

a. Use of Amplitude Response Envelopes

As indicated in Figure 6, the conventional flaw detection process has only three useful characteristics in the observed amplitude response envelope that can be used individually or collectively for the purpose of flaw characterization. These are the maximum amplitude, width of the amplitude response and the location of the maximum amplitude on the interrogating surface. The latter two are essentially amplitude independent flaw characterization techniques in the sense that they do not depend on the observed magnitude of the amplitude per se. In what follows are brief discussions of characterization techniques based on each of these three characteristics.

1) Maximum Amplitude

The most popular flaw characterization method makes use of the observed maximum amplitude. There are some variations as presented by the reference standard used. Side drilled holes, flat bottom holes and notches are examples of reference standards that may be produced in the structure being interrogated (internal standard) or in a separate block (external standard). Such references are suitable for establishing interrogation sensitivities. However, there are many instances where such reference standards are used for flaw size determinations by invoking the direct relationship between the amplitude and the reflector area. Assuming that the influence of flaw distance can be properly calibrated and/or corrected for, the misorientation of the flaw with respect to the beam renders the use of the amplitude/area concept invalid. The external standard has a further complexity since the attenuation is usually different from the structure under interrogation. A precaution for this situation is invariably reconciled by a statement that the attenuation should be the same. No mention is made of how one ascertains the similiarity in attenuation or what steps must be taken when a difference in attenuation is present.

Perhaps the greatest cause for concern in accepting the maximum amplitude as a measure of flaw size is the influence of the orientation of the flaw. As indicated by Wustenberg and Kutzner (5) it appears that for a transducer of approximately ½" in diameter, the maximum possible detectable flaw misorientation is about 10-15°. This assumes a detection threshold at 20 db below the amplitude noted from a 1/2" flaw oriented normal to the interrogating beam. Much the same observations have been presented by Haines. (78)

The advocates of the amplitude based flaw sizing technique underestimate the influence of the flaw misorientation by reasoning that the roughness and contour of the flaw surface substantially increases the angular distribution of the radiation from the flaw and thereby provides

an increase in the probability of detection. This is true, but the extent of the increase in the probability of detection is not appreciable. For the most part, the literature on the influence of flaw surface roughness has been concerned with the diffusivity of the ensuing radiation fields.[28,29] Kloth[30] has indicated that if the flaw has surface irregularities of less than a third of a wavelength, then the surface may be regarded as smooth. Working with a transducer with a center shear wave frequency of 2.25 MHz in steel, this amounts to surface irregularities of approximately 0.020". Coffey[30] also agrees that it is a matter of the ratio of the irregularities to the wavelength involved. He noted that below $\lambda/5$ the sound is considered to be scattered incoherently. Above $\lambda/5$ the coherent component of the beam will travel in a specular direction which means that there is no enhancement of detection due to surface roughness. Haines[78] suggests that the surface roughness may only be neglected when the roughness is less than $\lambda/20$. Haines and Langston[6] have experimentally studied the effects of surface roughness of reflector in a liquid medium; see typical data in Figure 14. The data was obtained by tilting the reflector once the maximum reflection was noted when the transducer and reflector were perfectly aligned. Since the centermost portion of the radiation from the transducer is always in use, the observed amplitude is characteristic of the reflector. Since the radiation field rotates two degrees for every reflector degree of rotation, it follows that if the indicated tilt angle is doubled the data may be interpreted as the directivity function of the reflector. The plotted solid line is the predicted reflected amplitude based on their modelling of the reflection process. The experimental points and their attendant range of values are also indicated. The reflector with a surface roughness of less than 5 um may be taken as a smooth reflector. It should be noted that the maximum amplitude drops by a factor of 12 db for an RMS surface roughness of 41 μm or $\lambda/8$ as compared to the wavelength of water at 5 MHz. At extreme divergence angles there is very little difference (≈2db) in the radiation of the two reflectors. This indicates that there is no additional incoherent scattering of the reflected radiation due to surface roughness. From the standpoint of reliability it seems more reasonable to design an interrogation procedure based on the probable occurrence of flat and smooth flaws since they are more difficult to detect.

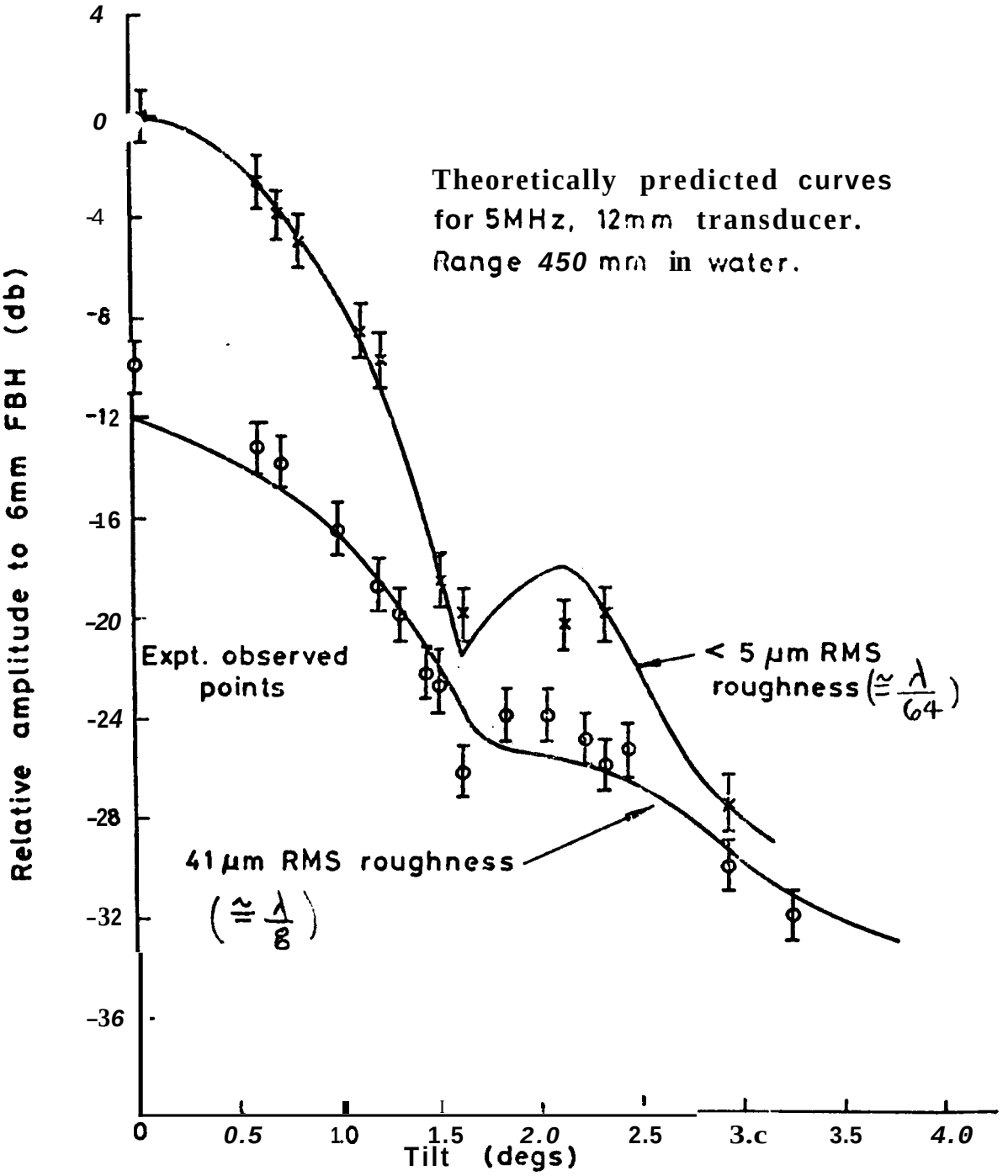

Figure 14 - Influence of surface roughness upon the radiation from a 6mm diameter reflector in water at 5 MHz. The independent variable is the reflector tilt angle. After Haines and Langston (6).

There have been a number of measures adopted in an endeavour to increase the reliability of the amplitude based flaw detection processes. The more important ones may be listed as the use of focused ultrasonic beams and tandem transducer systems, and the application of corrections to obviate the effects of those parameters that affect amplitude degradation.

The tandem system is diagrammed in Figure 15. [32,33] The technique is primarily for the detection of those flaws oriented nearly normal to the interrogating surface. As shown, detection is accomplished by two transducers whose separation is determined by the depth at which interrogation is desired. For such nearly normally oriented flaws, the amplitude would be the same as for detection by a single transducer with a zero misorientation. As to be expected, amplitude degradation will occur when the reflector is rotated from this orientation. However, the tandem technique does present the opportunity to detect a range of flaw orientations which cannot be detected by a single transducer angle beam.

In focused beams [34] the notion is that if one strikes the flaw with more ultrasound the probability of detection will increase. As previously stated there are two requirements for successful ultrasonic flaw detection, i.e., you must hit the flaw with ultrasound and you must get some back. Any improvement of flaw detection capabilities must cater to both of these requirements. The use of focused transducers as presented by contoured surfaces or arrays does not alter the second requirement. As Wustenberg and Kutzner [5] point out, for the same given range of misorientation angle, the single transducer and the tandem system are more suitable than focused beams; see Figure 16.

A more realistic approach in the use of amplitude data would be to consider corrections to the observed amplitude. These corrections would minimize the effect of amplitude degradation. In effect, one would attempt to approach the function F_1 of Equation 2 by eliminating the influence of the parameters of the other two functions. For example, if the misorientation angle is determined, its contribution to the amplitude

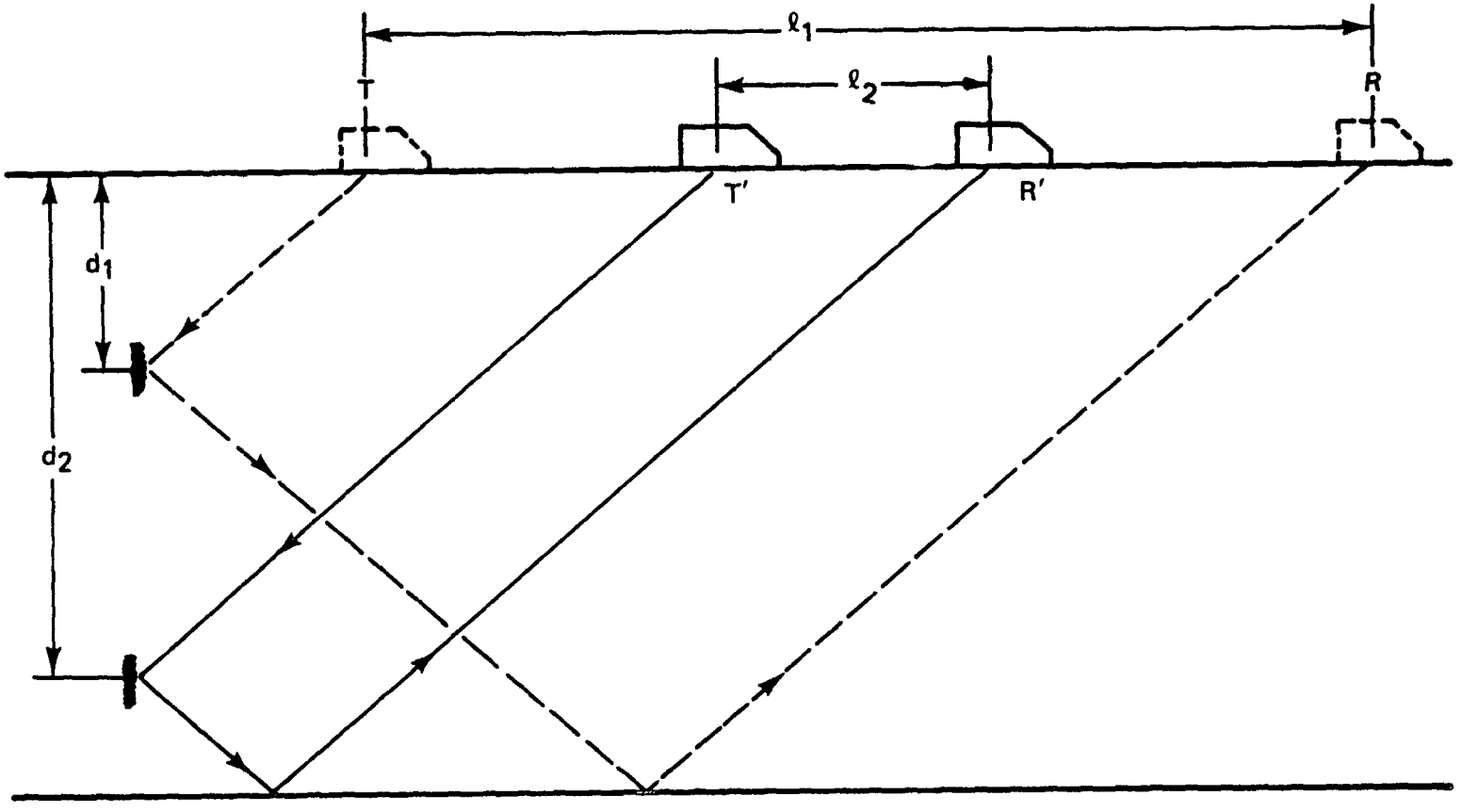

Figure 15 - The distance between the transducers for a given entry angle in the tandem angle beam technique is determined by the reflector depth.

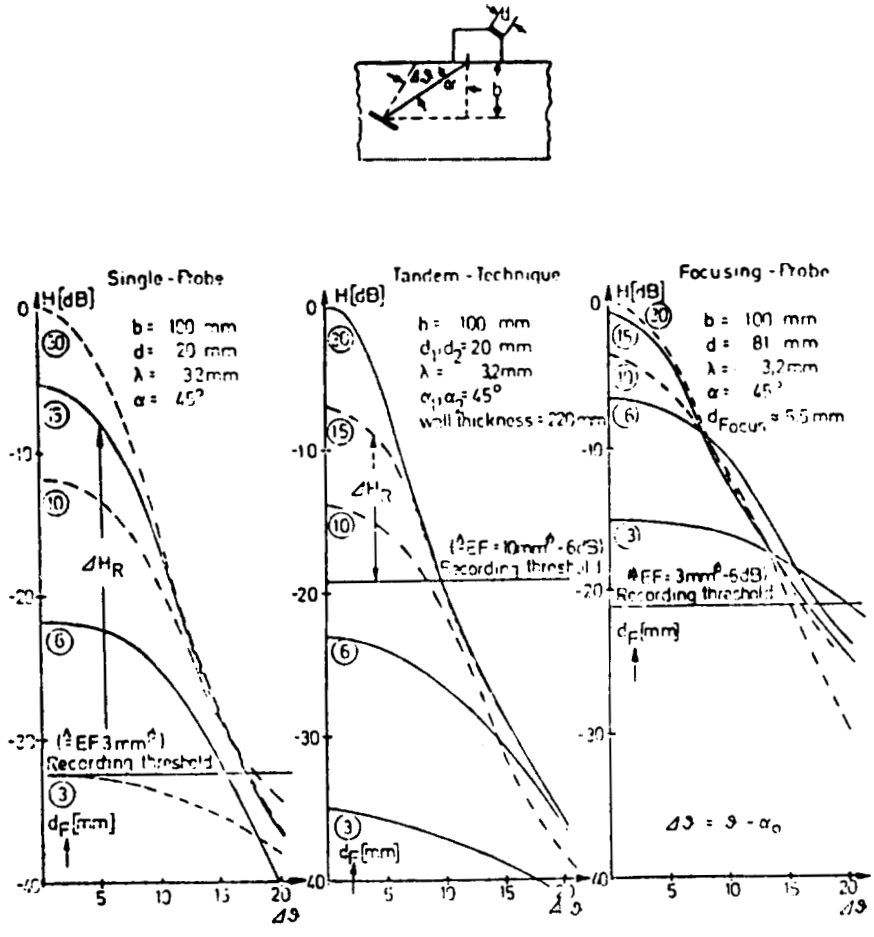

Figure 16 - The influence of the reflector size and misorientation upon the detectable maximum amplitude for interrogations by a single transducer, two transducers in tandem fashion and for a single focused transducer. After Wustenberg and Kutzner (5).

degradation can be formulated and eliminated. The other corrections would stem from the effect of flaw distance, attenuation and the standard used. An example of this concept is provided by Serabian (35) which deals with the determination of flaw size in large rotor forgings used for steam turbine-generator sets. It was found that such corrective measures can account for up to two orders of magnitude change in the observed maximum amplitude response. Needless to say, corrections due to flaw surface and contour cannot be applied. Thus, the determined flaw size must still be viewed as a minimum flaw size. However, such size determinations are immeasureably better than those obtained by using any evaluation process which directly uses the uncorrected amplitude data. The methods for making and applying such corrections have been available for some time, thus it is difficult to envision why more use has not been made of this data-correcting concept.

2) Width of the Amplitude Response Envelope

A relatively popular technique (9,36) adopts the projected distance ($\Delta\chi$) between two specified amplitude reference points on either side of the maximum along the scan line as the dimension of the flaw; see Figure 17. In the latter, the 6 dbdown or half amplitude points are used as the amplitude reference points. The 20 dbdown points as well as the points where the amplitude completely vanishes are also used. (37,79) The technique is valid when the flaw is much larger than the interrogating beam at the detection plane. As shown in Figure 18, the uncertainty of locating the end points of the flaw becomes a minor part of the total measurement of the flaw size or length in the direction of the transducer motion. The reflection from the flaw is purely geometric in nature and is essentially void of diffraction effects. This is not the case when the flaw is smaller than the beam. Under this condition the detection process is totally dependent upon the spatial interplay of the radiation fields from both the flaw and the transducer. (38) The problem has been studied with this premise. (21) The width ($\Delta\theta$) of Figure 17 of the amplitude response

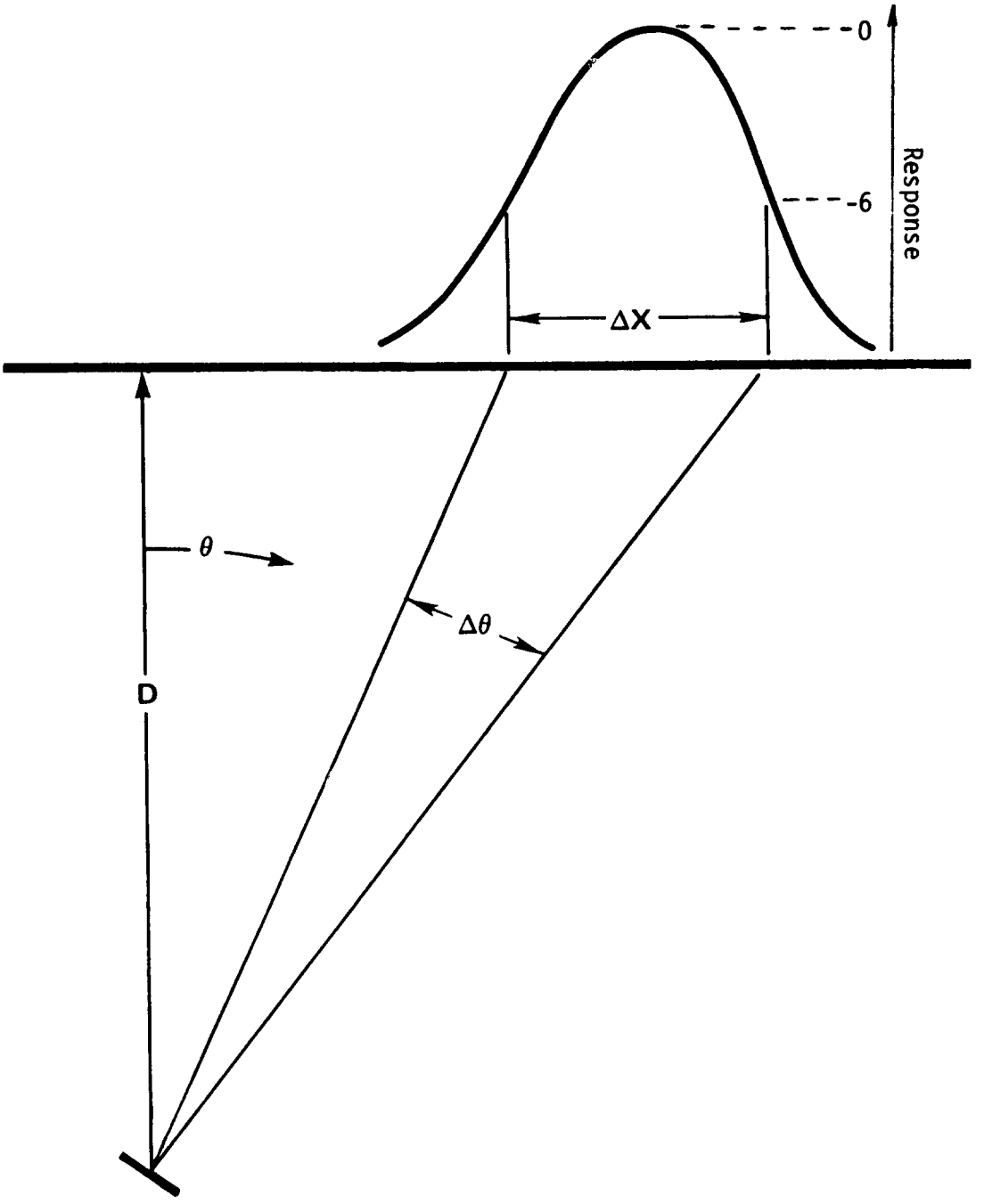

Figure 17 - Me surable characteristi (AX and Δθ) of the width of amplitude response envelopes; use of the -6 db amplitude decay points are illustrated. After Serabian and Lawrie (21).

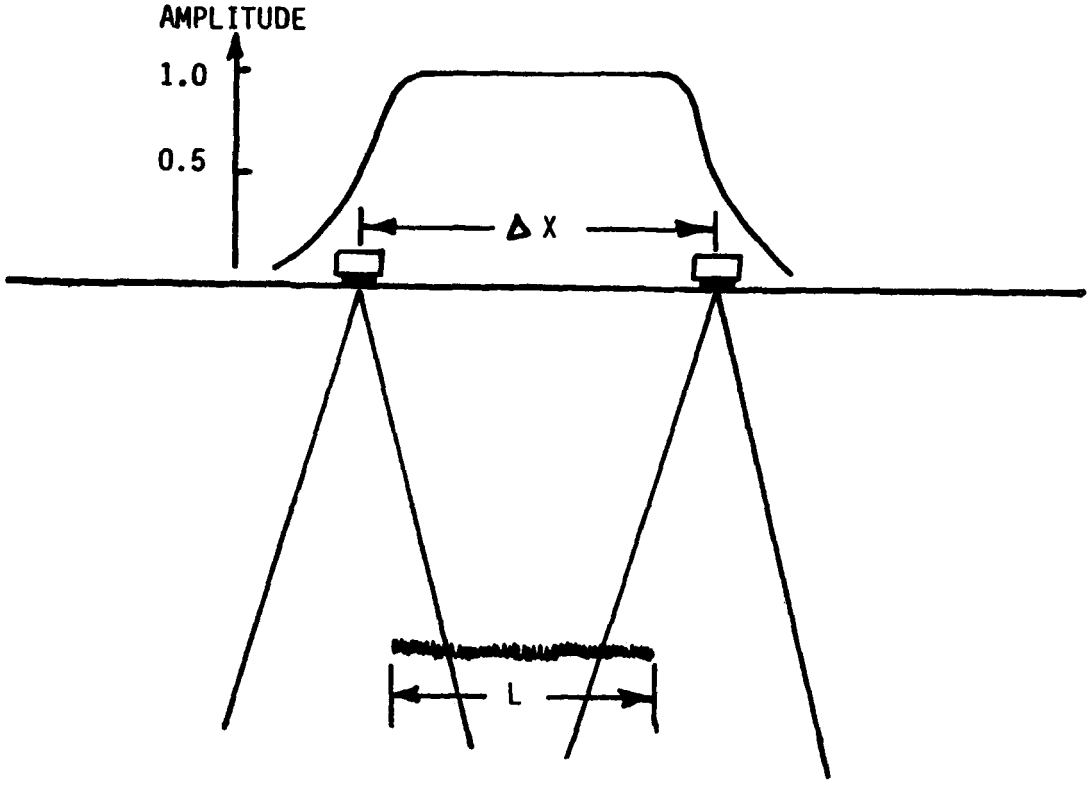

Figure 18 - Using specified amplitude decay points (-6 db points shown) for estimating the size of flaws that are larger than the beam on the detection plane. The determined size (AX) is invariably larger than the true size (L).

envelope was monitored by the amplitude decay at the 6 db down points from the maximum amplitude points. The calculated results for a misorientation angle of 5^{o} are shown in Figure 19. As expected, the width of the amplitude response envelope is a function of both the transducer and reflector sizes, The proponents of this sizing technique attempt to delete the influence of the transducer by subtracting the beam width at the detection plane. It is evident that the subtraction of a constant width representing the transducer beam width would not detract from the observed fact that the width of the amplitude response envelope for a given size transducer decreases with flaw size and/or orientation.

From Figure 17, it is also evident that any flaw size determination which depends on an amplitude response envelope is influenced by the depth of the flaw. Figure 20 indicates this effect for a flaw at a misorientation angle of 10^{o}. Working with a 1/2"-2 1/4 MHz transducer, 1/4" and 1" flaws at a depth of 4 inches would be sized as 0.72" and 0.28", respectively. The error involved is usually to overestimate the smaller flaws and underestimate the larger flaws, The latter is the more harmful result in that an optimistic stance is adopted for the flaw content of the material or structure being evaluated.

3) The Location of the Maximum Amplitude

The location of the maximum amplitude of the amplitude response from a misoriented flaw is determined by the sizes of the transducer and reflector involved. (39) Figure 21 indicates this concept. Assume that the reflector size of diameter $(n\lambda)$ is much larger than the transducer size $(N\lambda)$, so much larger that the transducer may be considered a point source. Under this condition the radiation field of the reflector is responsible for the location of the maximum amplitude. This is shown for both the straight and angle beam on the top half of Figure 21. It should be noted that when $n>>N$ the location of the maximum amplitude in terms of the scanning parameter (θ) of the flaw detection model of Figure 3, approaches the misorientation angle. When $n<<N$ it is the radiation field of the transducer that is responsible for the

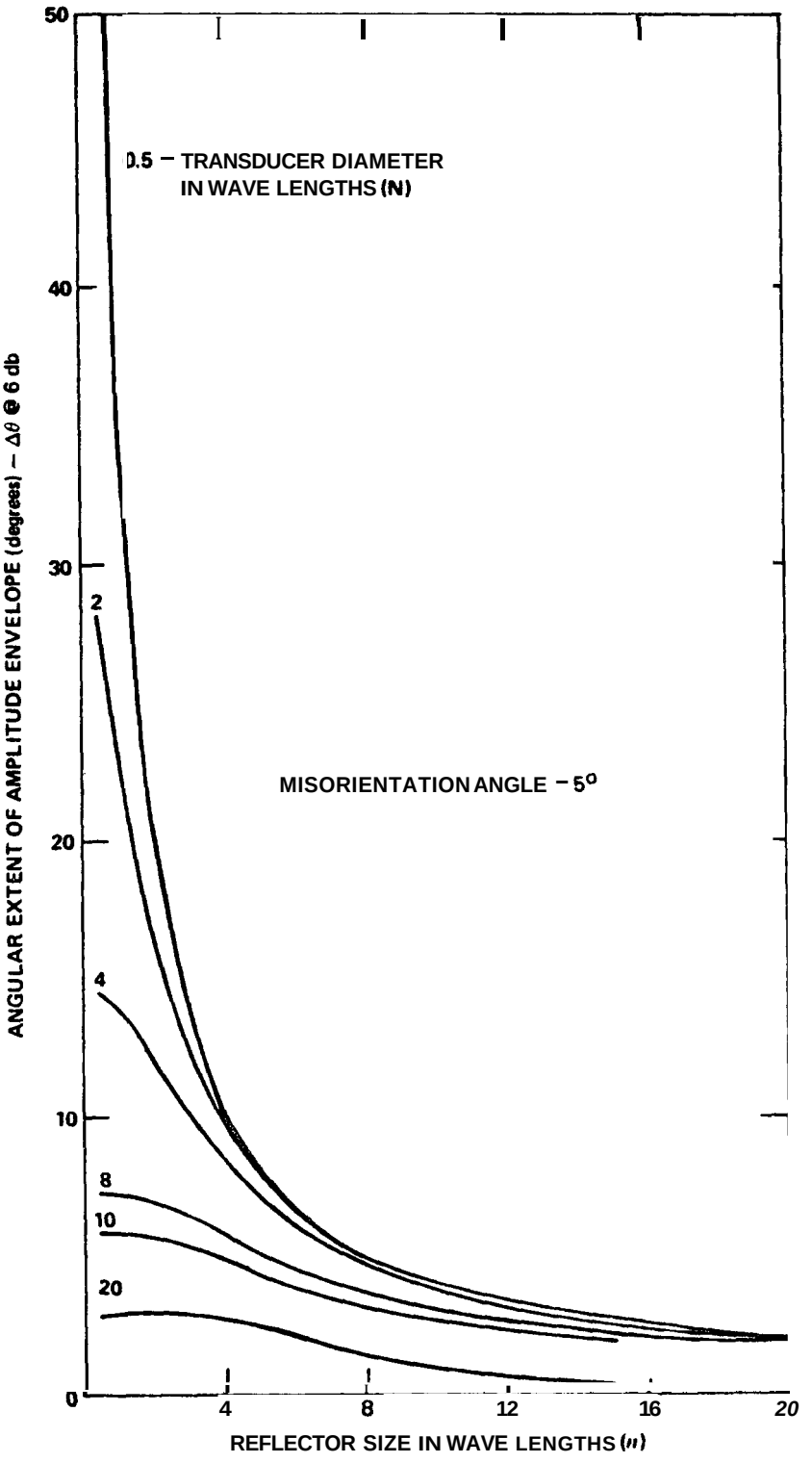

Figure 19 - Width of the amplitude response envelope at the -6 db decay points as a function of the transducer and reflector sizes; reflector misorientation is five degrees. After Serabian and Lawrie (21).

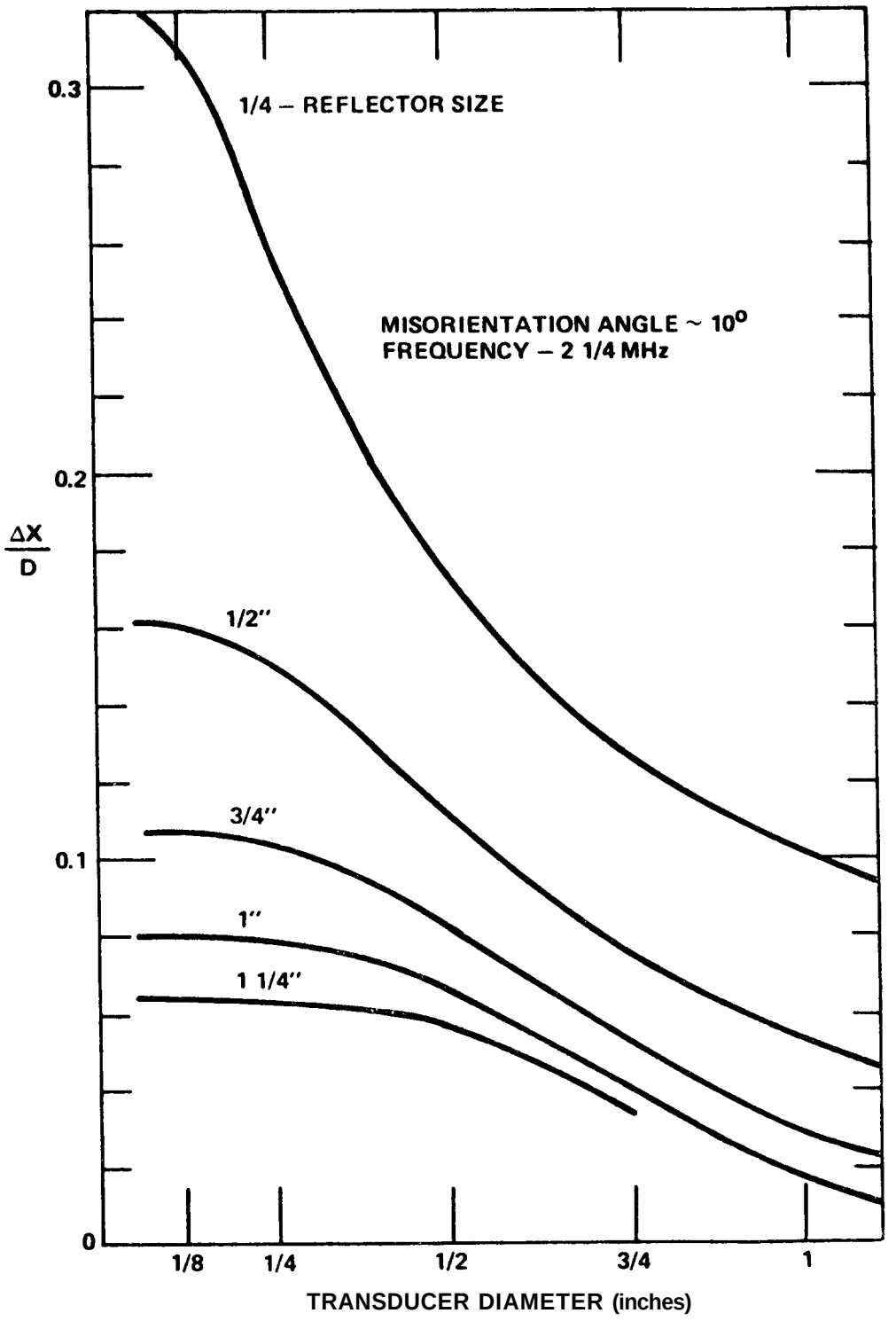

Figure 20 - Reflector size determinations using the projected -6 db decay points of the amplitude response envelope. AX is the width of the amplitude response envelope between the -6 db points; D is the depth of the flaw. After Serabian and Lawrie (21).

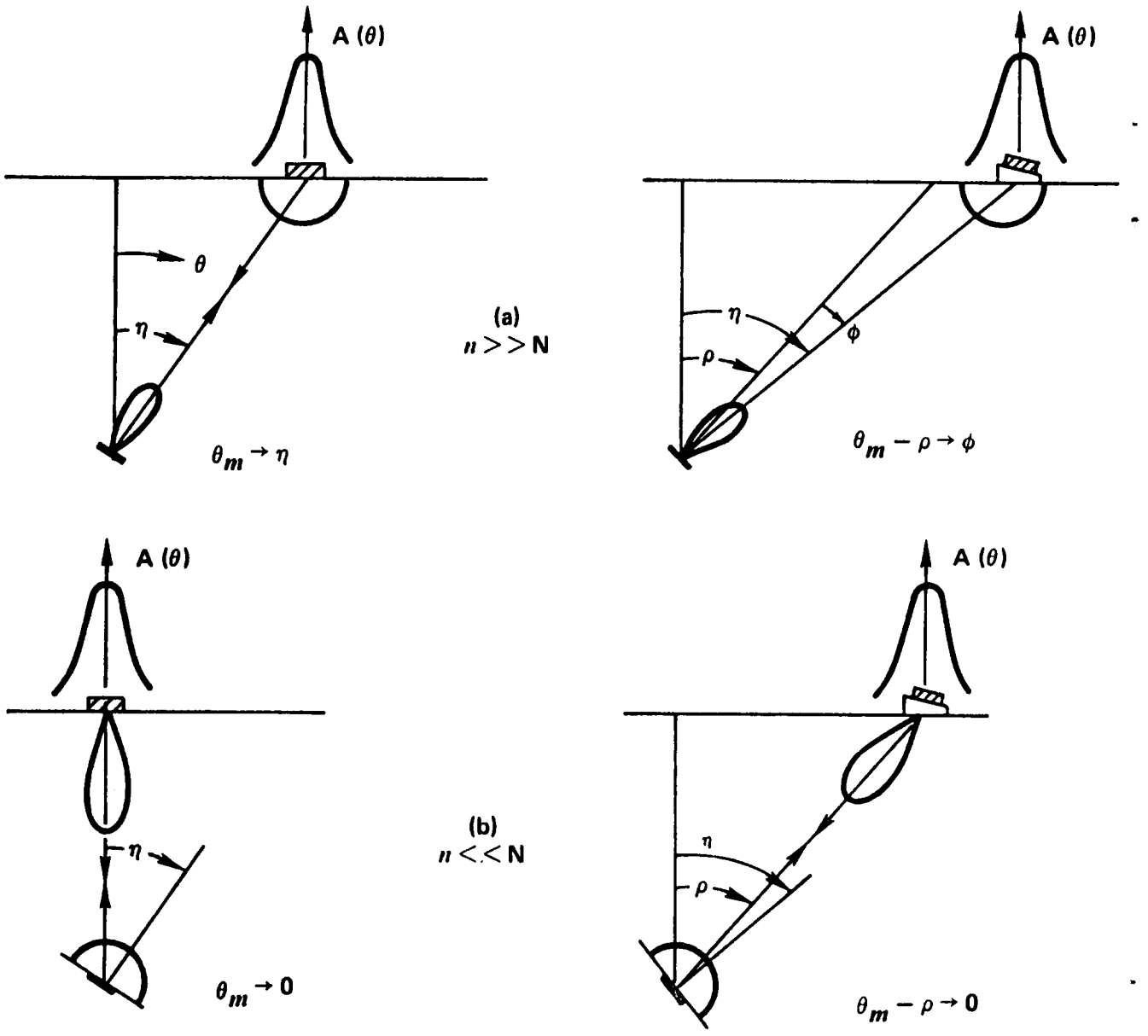

Figure 21 - Extremes in the location of the maximum amplitude for the straight and angle beam interrogations. After Serabian and Lawrie (39).

location of the maximum amplitude and θ_m approaches zero and ρ for the straight and angle interrogations, respectively; see bottom half of Figure 21. Figure 22 displays the location data for a variety of misorientation angles as determined by the detection model of Serabian and Lawrie.[21] Figure 23 shows experimental verification of this by using the blocks described in Figure 10.

Of prime importance is the display of Figure 22. It can be used to derive intelligence of the flaw causing the detected maximum amplitude. Assume that a transducer size of N_1 indicates a amplitude maximum location of θ_{m1}. As shown in Figure 24a, this could mean that the reflector has a size of n_1 and a misorientation of ϕ_1 or size n_2 with a misorientation of ϕ_2, etc. These possibilities are plotted in Figure 24b. If another (smaller) transducer of diameter N_2 is used, the resulting θ_{m2} would suggest a different set of flaw sizes (n_i) and their associated misorientations (ϕ_i). This second set of data is also shown in Figure 24b and the intersection is representative of the true flaw size and misorientation. It is significant to note that these determinations of size and misorientation were made without recourse to the magnitude of the maximum amplitude. Moreover, a small amplitude response from a large adversely oriented flaw would be given equal status as a large amplitude response as created by a small favorably oriented flaw. It should be noted that the orientation of the flaw is also determined. It is significant to note that since the location of the maximum is a function of relative sizes of the reflector and transducer only, such determinations are independent of frequency. Figure 25 indicates experimental support for this observation.

This procedure has had no field evaluation with natural flaws as yet. However, the proven experimental success of the model to date indicates great promise for this novel flaw characterization technique.

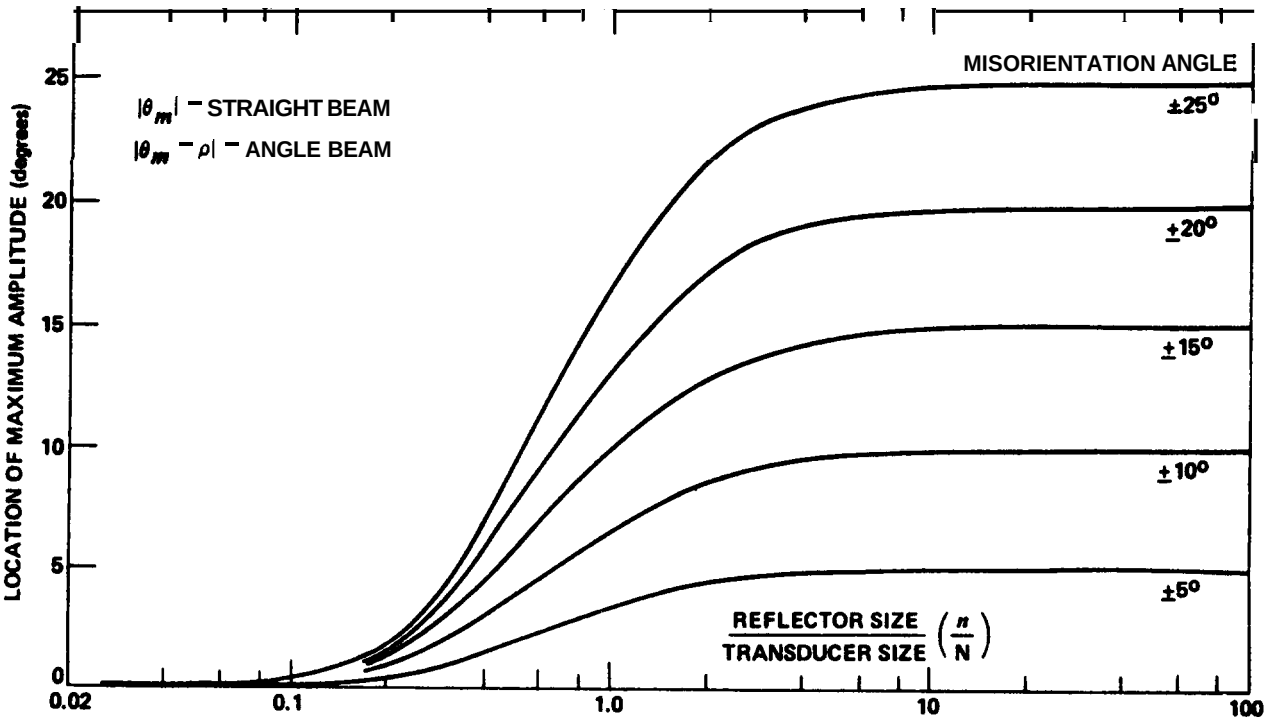

Figure 22 - Location of the maximum amplitude in terms of the ratio of the reflector to transducer sizes. After Serabian and Lawrie (39).

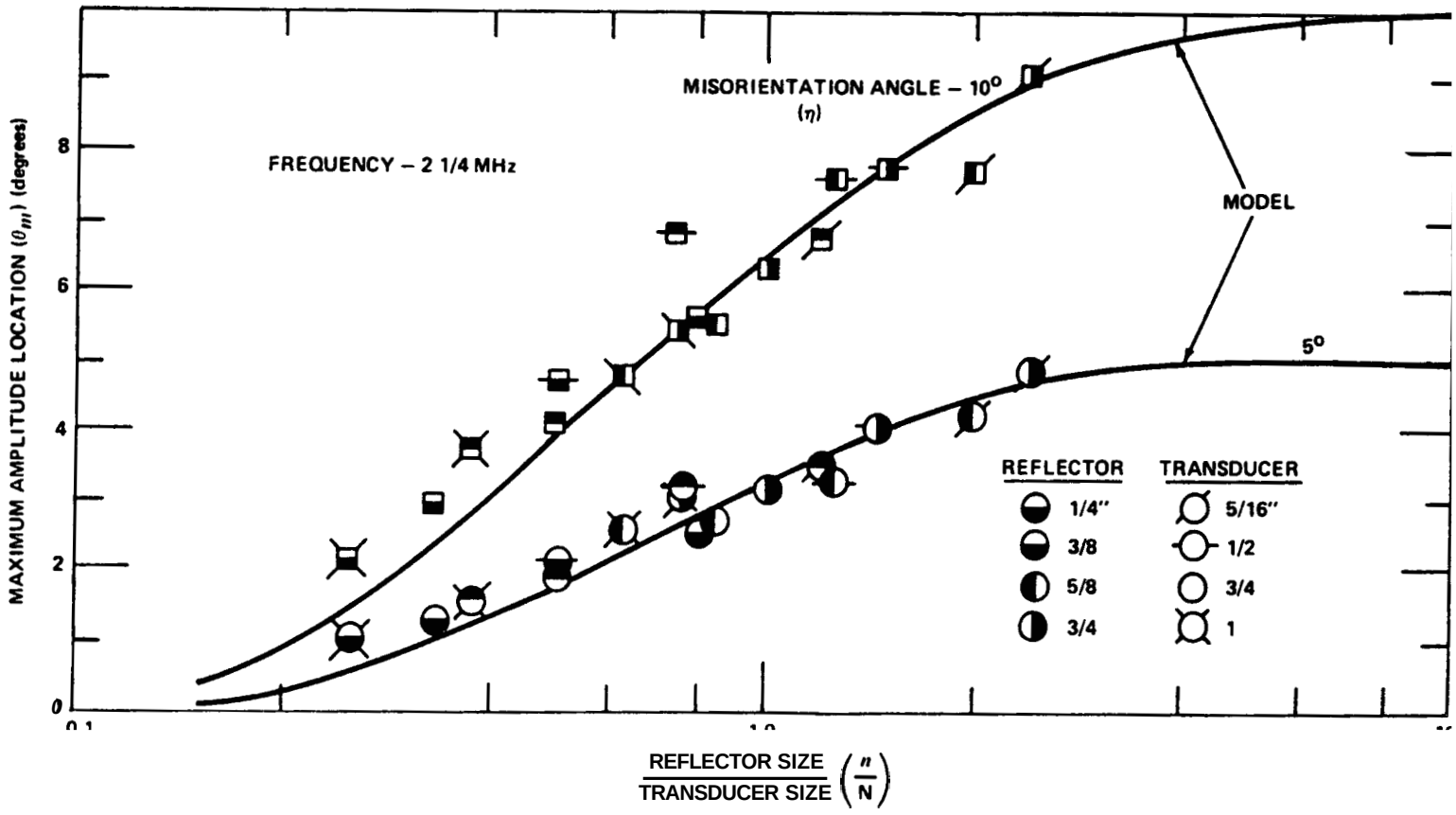

Figure 23 - Experimental data on the location of the amplitude maximum in terms of the ratio of the reflector and transducer sizes; two different reflector misorientations are shown. After Serabian and Lawrie (23).

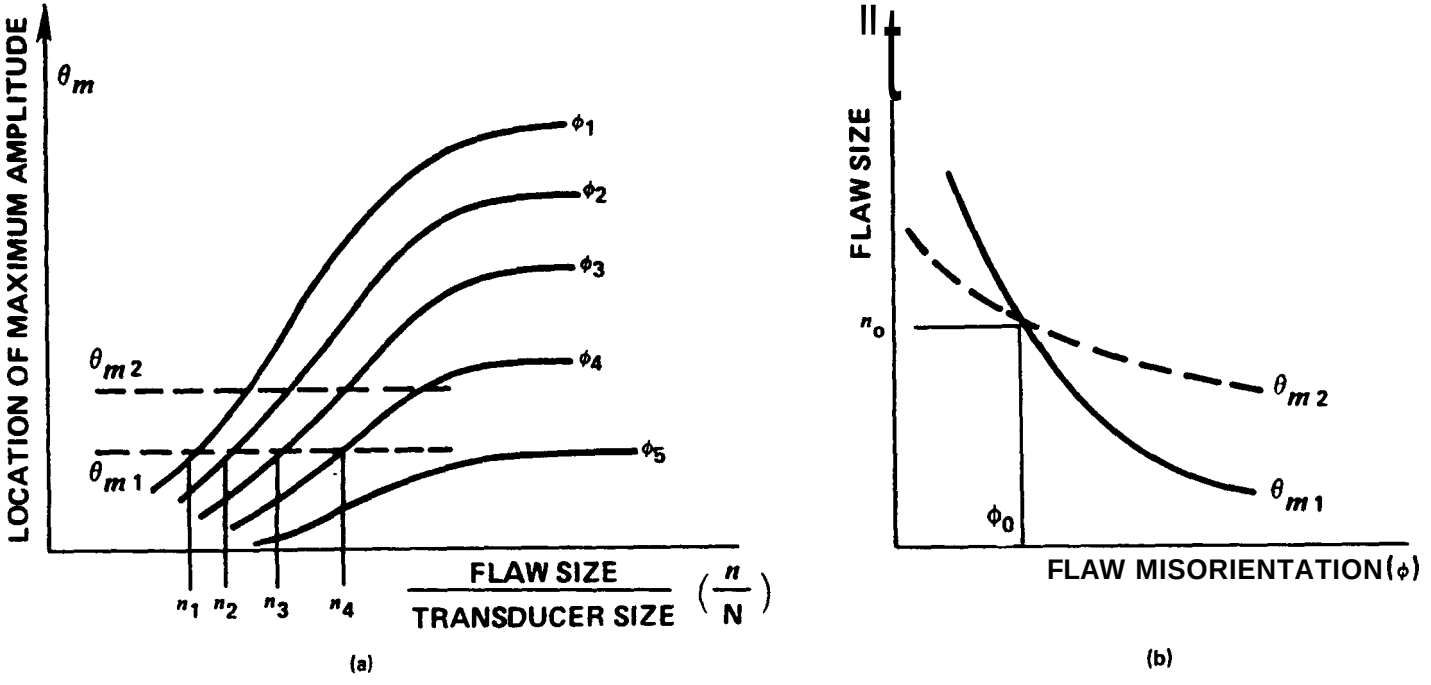

Figure 24 - Determination of the true flaw size (n_o) and its associated misorientation angle (ϕ_o) by the use of the location (θ_m) of the maximum amplitude, The intersection of two such location measurements made with different transducer sizes is involved. After Serabian and Lawrie (39).

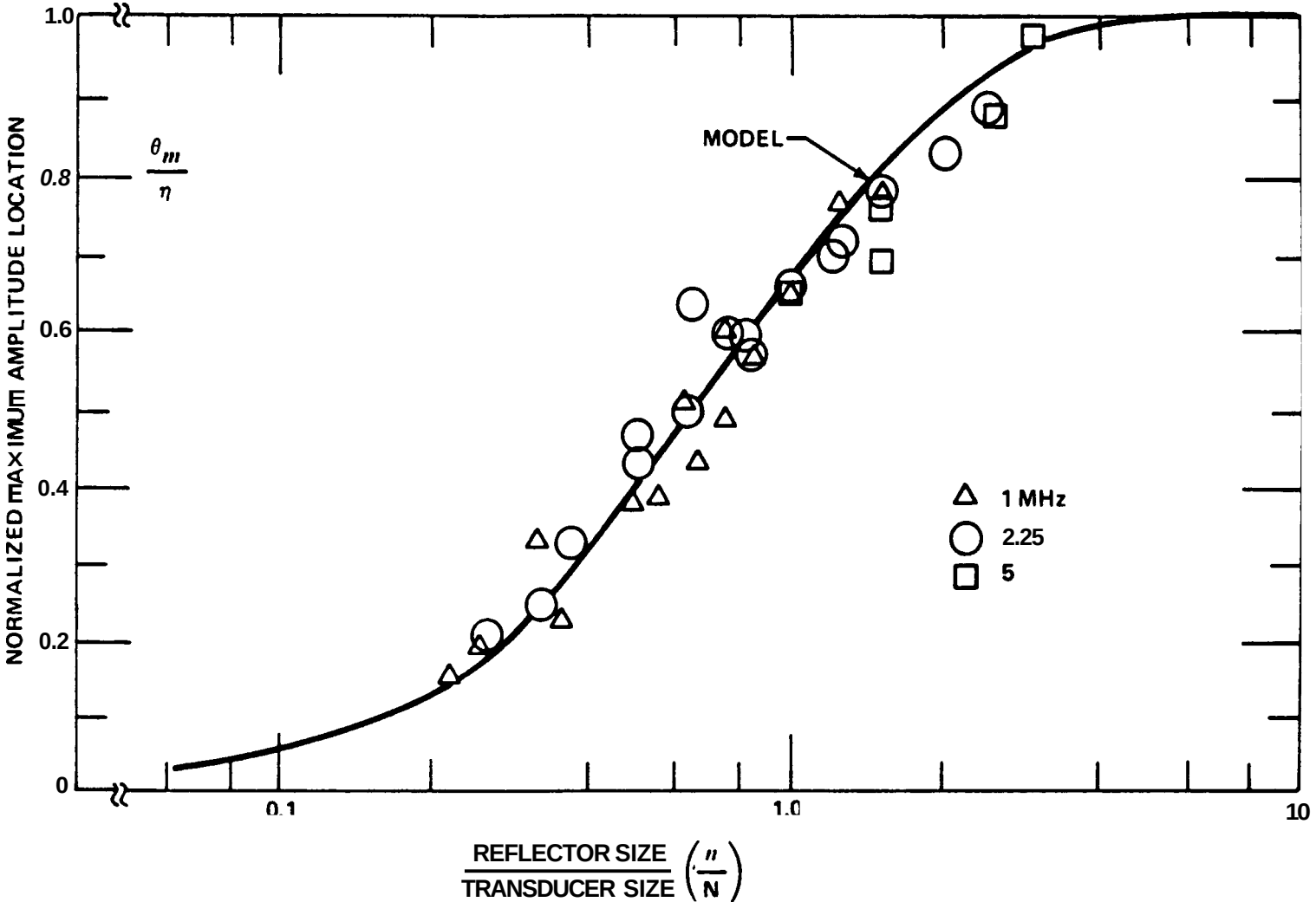

Figure 25 - The location of the maximum of an amplitude response envelope is independent of frequency. After Serabian and Lawrie (39).

b. DGS Techniaue

The distance-gain-size (DGS) technique is used quite extensively in Europe.[40] The technique attempts to relate flaw distance, gain of the flaw amplitude above a standard amplitude and the flaw size involved. The approach is to formulate the amplitude of ultrasound that strikes the flaw which then becomes the source of the radiation back to the interrogating transducer. In the far field of radiation this formulation makes use of the pressure field generated by a piston source oscillating in semi-infinite space. The near field radiation is determined experimentally with the use of reflectors in water. The amplitude of ultrasound from the back wall on the side opposite the transducer is determined experimentally and used as a reference standard. Figure 26 shows the amplitude data plotted in terms of near field lengths. The latter permits the use of such displays for any transducer size or frequency as well as any flaw distance and specimen thickness. Of particular interest is that the back reflection is used as the standard which eliminates the need for artificial reflectors such as side drilled or flat bottom holes. The procedure is, first, to determine the db difference in amplitude between the flaw and back surface reflections. This difference is plotted at the appropriate back surface distance; see point 1 of Figure 26. A lateral shift to the flaw distance moves the point to a particular amplitude-distance curve (point 2), thus allowing one to read the flaw size in terms of the transducer size.

Opel and Ivens[41] proposed a procedure to correct for material attenuation. The measurement procedure assumes that the ultrasonic beam is void of diffraction effects and has a uniform intensity at any point within a given cross section. The correction is independent of frequency and the true worth of the correction has never been adequately evaluated. There are many other suitable techniques for the measurement of attenuation that are based upon principles more in line with realistic physical concepts.

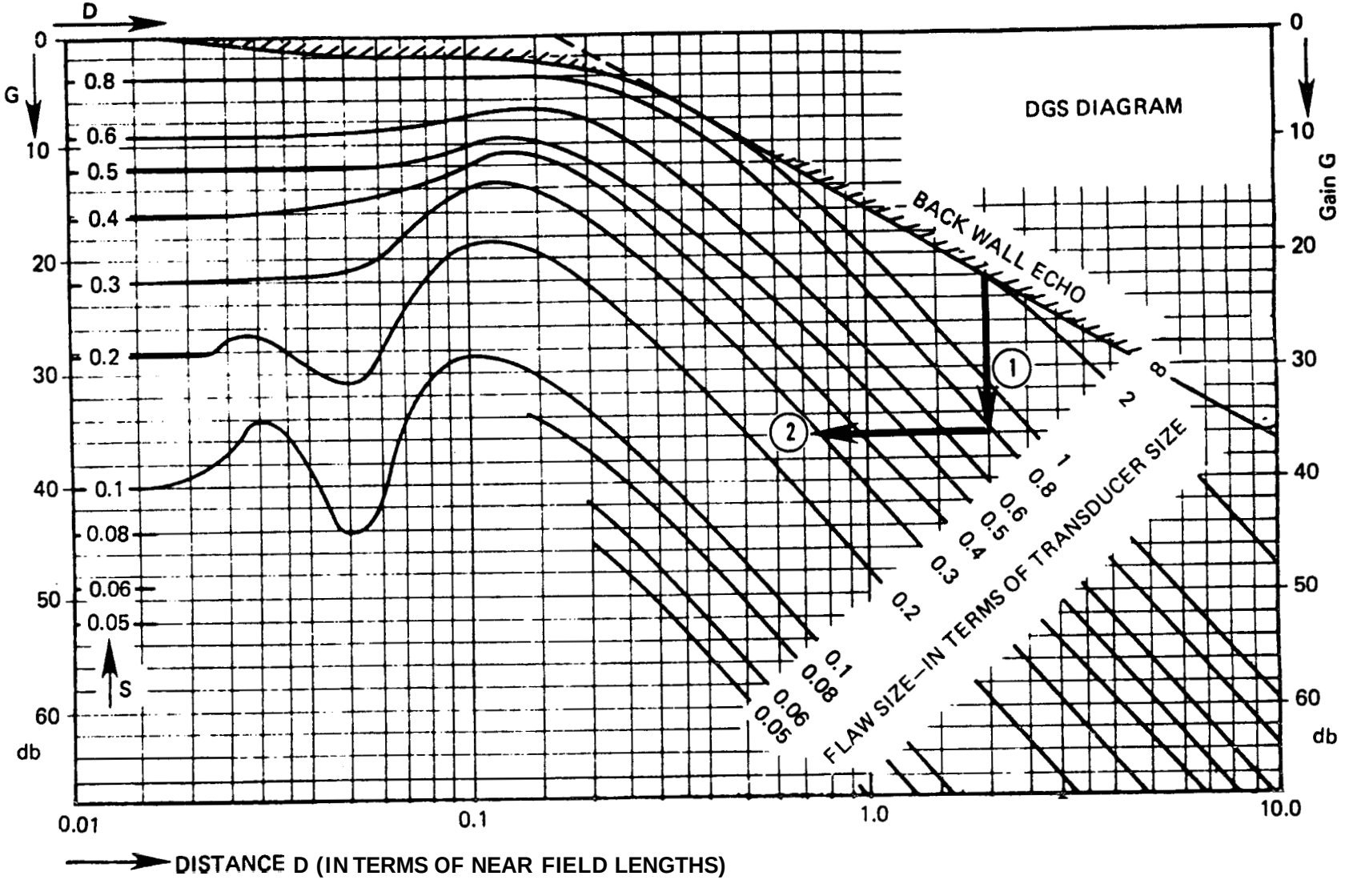

Figure 26 - The distance-gain-size (DGS) technique of flaw sizing. Point 1 represents the amplitude difference between the flaw and the back reflection; the amplitude difference is plotted at the back reflection distance. Point 2 is the translation of point 1 to the appropriate flaw distance, thus facilitating its location on a particular amplitude-distance-size curve. The size may then be read in terms of the transducer size. After Krautkramer (40).

DGS diagrams have been modified for use for both angle beam and for the double transducer or tandem procedure of interrogation.[42] The DGS technique of flaw characterization has some merits in that it has generalized application in terms of transducer sizes, frequency and flaw distance. However, it does not take into consideration the misorientation between the flaw normal and the interrogating beam. For this reason the technique is limited in its application. The German Commission on NDT has taken steps to eliminate the connotation that the use of the DGS technique can determine flaw size. They have adopted the use of the phase "Reflectivity Diagrams" for DGS diagrams.[43]

c. Ultrasonic Spectroscopic Techniques

Since 1963[44] there has been an increasing interest in the use of ultrasonic spectroscopic techniques for flaw characterization. In essence, one analyzes the characteristics of the frequency content in the radiation from a reflector or flaw which has experienced an incident pulse consisting of a broad band of frequences. The flaw, by virtue of its size, orientation, shape, surface roughness and contour, generates selected interference-produced maxima and minima in the resulting reflected radiation. The initial work[45,47] considered the Bragg type interference phenomenon while the most recent work[48] utilizes the interference minima of amplitude-frequency-direction spectra.

The use of Bragg type interference presents a means of determining flaw size and orientation. This would permit one to correct for the effects of flaw orientation in any amplitude-dependent flaw characterization process. The analysis is based upon the interference resulting from the superposition of the spherical wavelettes emanating from the opposing extremes of the reflector. As shown in Figure 27, the total path length difference, $2(2b)$, which is well into the far field of radiation, is given by $2d\sin\theta$. The constructive interference condition may be written as

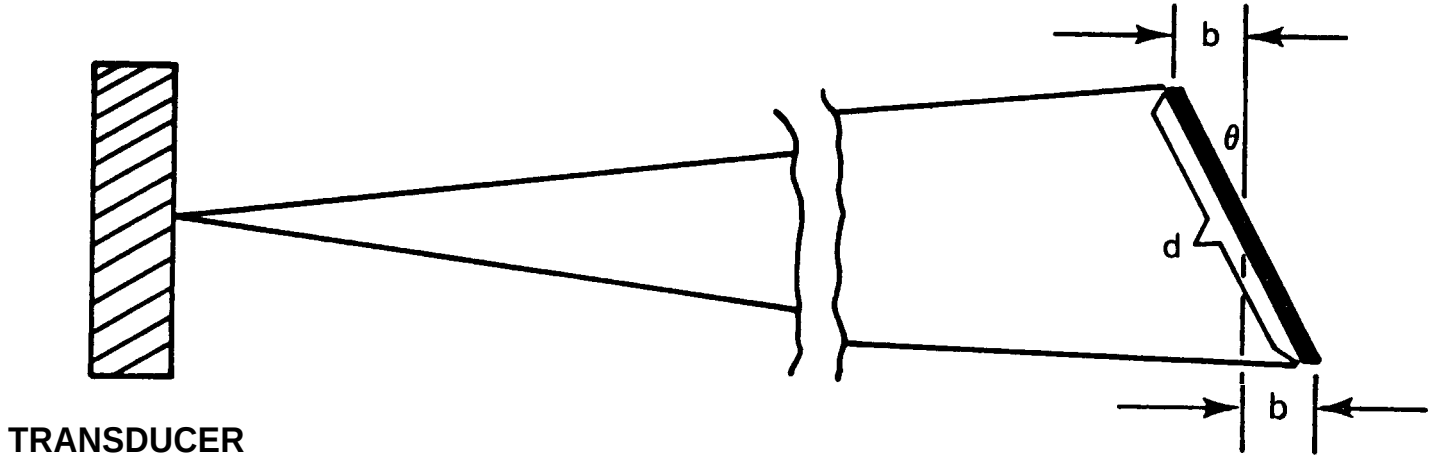

Figure 27 - The path length difference of the spherical wavelets emanating from the reflector extremes produce a phase-induced interference mechanism at the interrogating transducer. Far field of radiation is considered. After Whaley and Adler *(45)*.

$$2d\sin\theta = n\lambda = \frac{nV}{f} \qquad (3)$$

where λ is the wavelength and n is the order number. At interference conditions the spectral content of the returned pulse packet will take on the characteristics indicated in Figure 28. As an example, consider a flaw 0.250 inches in diameter at an orientation angle of 30^{o}, thus

$$2d\sin\theta = .250 = n\lambda \qquad (4)$$

Constructive interference would occur at λ = 0.250, .125, .063, .032, .016, ... or at frequencies of 1.0, 2.0, 3.96, 7.8, 15.6 ... These frequencies are realistic interrogation frequencies when one considers the prevalent use of broadband transducers.

Of prime importance for flaw characterization is the frequency interval (Af) between consecutive frequency peaks. From Equation 3, this frequency interval becomes:

$$Af = \frac{V}{2d\ \sin\theta} \qquad (5)$$

By using the two transducer configuration indicated in Figure 29, the frequency intervals observable at receiving points 1 and 2 are given by (47).

$$\Delta f_1 = \frac{V}{d\left[\sin(\theta \pm \alpha_1) + \sin\theta\right]}$$

$$\Delta f_2 = \frac{V}{d\left[\sin(\theta \pm \alpha_2) + \sin\theta\right]} \qquad (6)$$

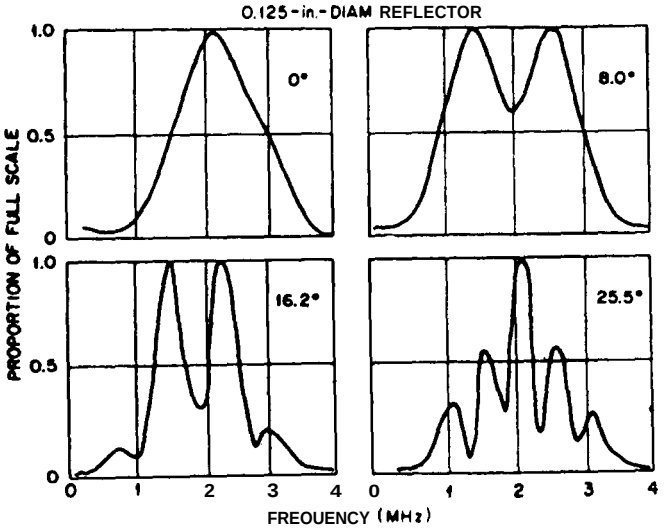

Figure 28 - Ultrasonic frequency spectra for a 0.125 inch diameter reflector at various angles of orientation. After Whaley and Adler (45).

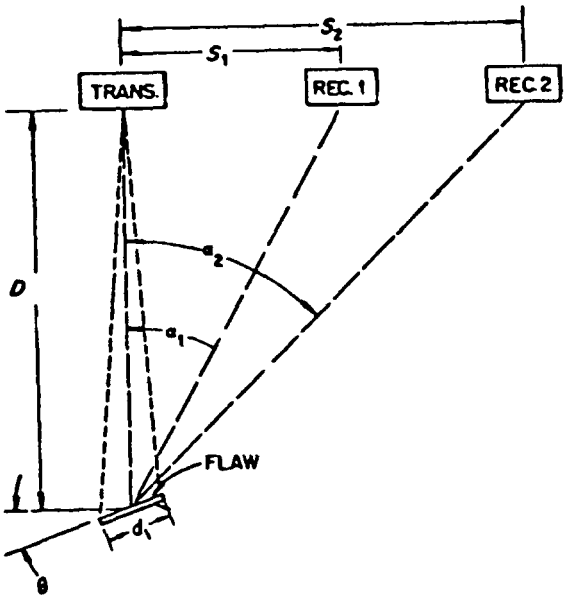

Figure 29 - Geometric parameters for calculating flaw size by the use of ultrasonic spectra. After Whaley and Cook (47).

where each angle a is computed from known D and S distances. Solving the above equations will yield both the flaw size (d) and its orientation (θ). No inference is made regarding the shape of the flaw, thus the size determined pertains to the flaw length in a plane containing the transducers and flaw. Therefore, one should consider at least two orthogonal directions. In this manner, a more realistic evaluation of size and orientation would be obtained. Figure 30 [80] presents a measure of the excellent success of this technique. The work of L. Adler et al [49] summarizes the use of the technique for the evaluation of weldments by the immersion method. The presence of the water buffer necessitated changing the frequency interval equations as stated above.

Johnson [81] has adapted the work of Neubauer [82] to generate a model for the interference effects observed by Whaley and Adler. The model is based on Huygen's optical principle. Each point is considered to be a secondary spherical source whose contribution at the transducer must be summed with due regard to amplitude and phase. The model has been able to predict the positions and the number of maxima and minima of the reflector-modulated frequency spectra of Figure 28.

Another interference technique [48] makes use of the fact that the directivity function of a transducer may be interpreted as either an amplitude-direction distribution for a given frequency or as an amplitude-frequency distribution for a given direction. Figure 31 indicates this notion for a rectangular transducer. As an application of this concept for flaw characterization consider Figure 32. A transmitter is located directly over the flaw to be evaluated. This location can be noted by the minimum flaw distance. Two observations are made at positions where frequency minima are observed; positions A & B. If it is established that these minima are not those of the transducer, then it ran be assumed that they are due to the flaw. With this in mind the first minima may be described by:

$$F_{1A} = \frac{c}{d_f \, \mathrm{Sin}(2\alpha - \phi_A)}$$

$$F_{1B} = \frac{c}{d_f \, \mathrm{Sin}(2\alpha + \phi_B)} \qquad (7)$$

where c is the velocity of propagation and F_{1A} and F_{1B} are the frequencies

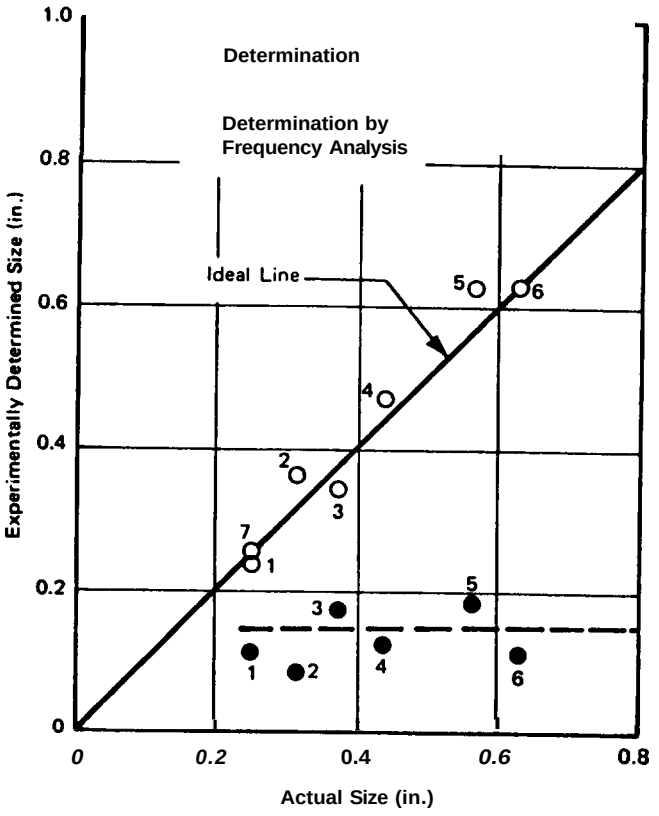

Figure 30 - A comparison of flaw sizing by the frequency analysis method (○ points) and the use of conventional amplitude considerations (● points). After Whaley and Adler (80).

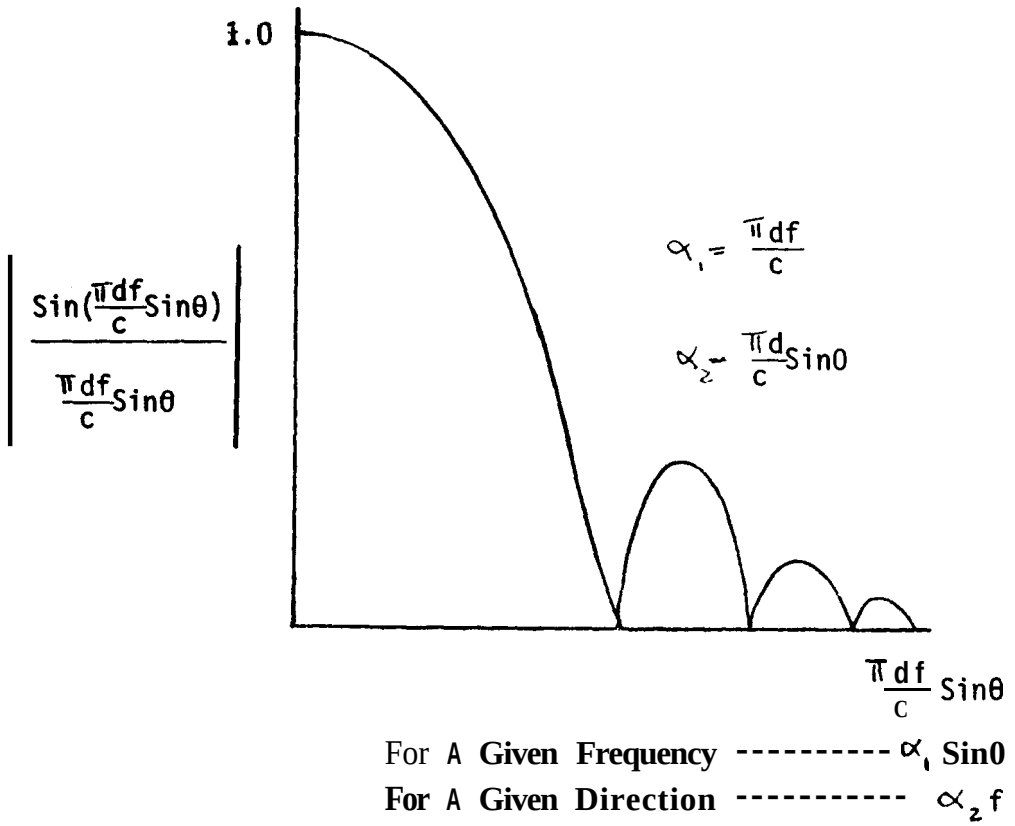

Figure 31 - The directivity function of a transducer may be interpreted as either an amplitude-direction distribution for a given frequency or as an amplitude-frequency distribution for a given direction. A rectangular transducer whose one dimension d is indicated.

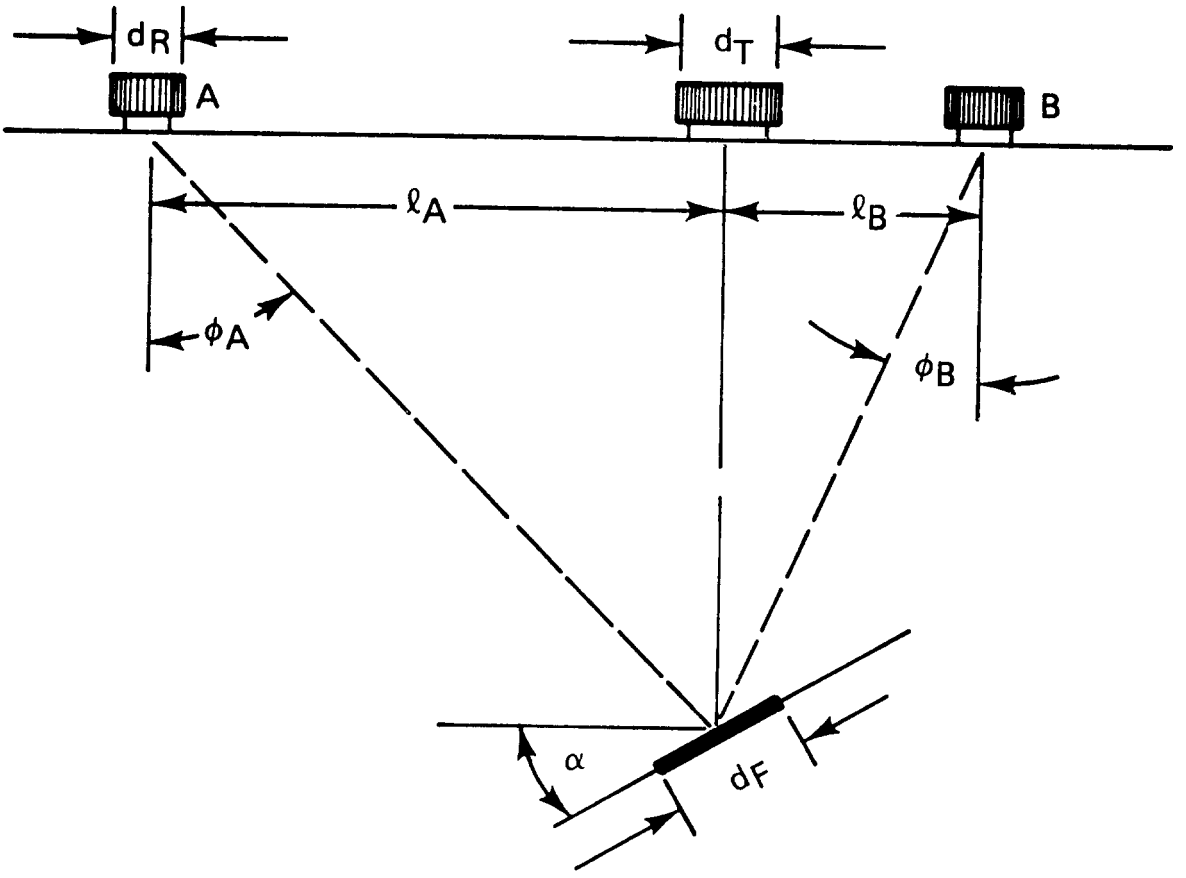

Figure 32 - Geometric aspects for flaw size and orientation determinations by ultrasonic spectroscopy.

of the first minima at positions A and B, respectively. Also, the angles ϕ_A and ϕ_B may be determined by the geometry of Figure 32. Solving the above equations will yield d_f and a which are the flaw diameter and orientation, respectively. As in the previous interference technique the size and orientation determinations are those in the plane containing the flaw site and the transducers. It is necessary to make at least four spectral measurements at two orthogonal directions for realistic flaw characterization. This characterization technique has been extensively evaluated as part of the work of this program. The reader is referred to Section VII.

d. The Delta Technique

The delta technique is a multi-transducer weld interrogation scheme suitable for both the contact and immersion modes. The technique is based upon the detection of redirected ultrasound, rather than the directed ultra-. sound of conventional detection techniques. Figure 33 [83] illustrates the various types of redirected ultrasonic energy and the manner in which such energy from a transmitter (T) can reach the receiving transducer (R). Three types of defects are shown; vertical smooth, spherical and a rough or natural defect. Figure 34 displays the basic transducer configuration for the immersion delta system and indicates the reason for the use of "delta" as a descriptive phrase; the transducers and flaw or radiation site form a triangle. As many as six transducers can be utilized with scan rates up to 50 feet per hour. [84]

The use of multiple transducers makes it possible to detect reflectors at orientations which can be unfavorable for the conventional single or double transducer assemblies. The interpretation of the observable results are dependent upon the separation(s) and the included angle(s) between the transducers. However, since the selection of the latter appears to be arbitrary, it is difficult to establish meaningful standards and references. Therefore, the delta interrogation procedure is not condusive to quantitative reasoning.

The literature [83,85] indicates that all normally encountered weld imperfections has been detected by the delta technique. Cross and Tooley [86] report better detecting ability than conventional ultrasonic techniques or

radiography. The latter is illustrated by Figure 35. Figure 36 is a metallographic examination of point A of Figure 35. However, these results cannot be interpreted as a general testimony for the abilities of the delta technique. One must admit that slight changes in the already arbitrarily selected geometric configuration of the transducers can conceivably obviate the indicated detection results.

The above remarks are attested by the fact that the literature is essentially void of any appreciable use of the delta technique since its introduction in 1967. It would appear that the delta technique has unique abilities as an auxiliary interrogation scheme. In its present form, the ability of the delta technique for flaw characterization is qualitative at best and does not seem to be applicable to quantitative assessments.

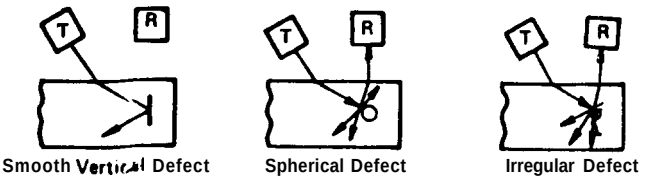

a. Reflected Energy

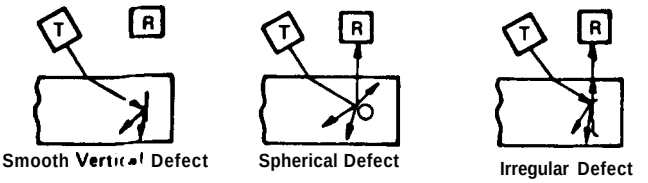

b. Mode Converted Energy (Direct)

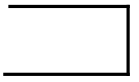

c. Mode Converted Energy (Indirect)

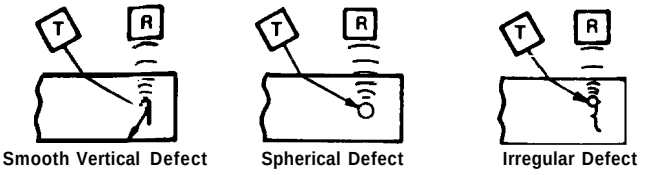

d. Reradiated Energy

Figure 33 - Various modes of propagation of redirected ultrasound from a flaw. After Cross et al (83).

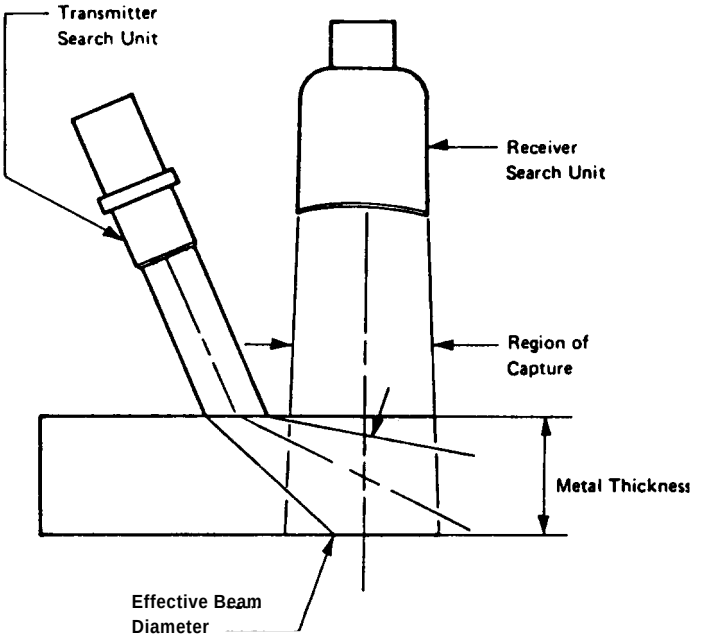

Figure 34 - The basic delta interrogation configuration. After Cross and Tooley (86).

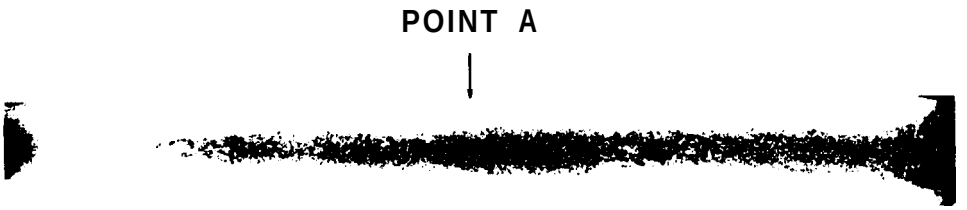

RADIOGRAPH

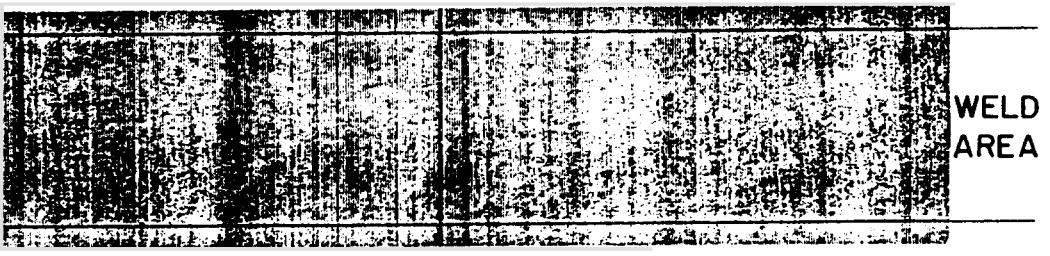

60° SHEAR WAVE RECORDING

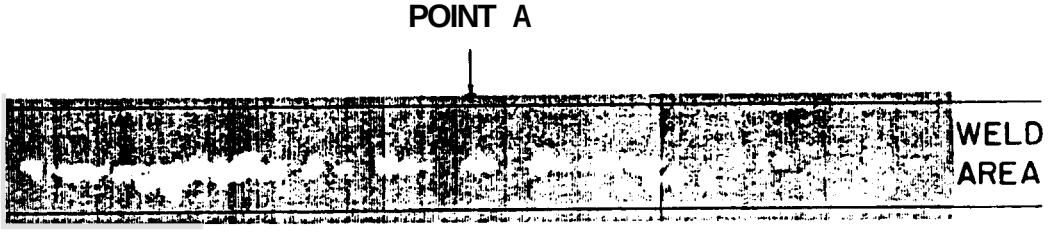

DELTA SCAN RECORDING

Figure 35 - A comparison of the delta scan technique with conventional ultrasonics and radiography. After Cross and Tooley (86).

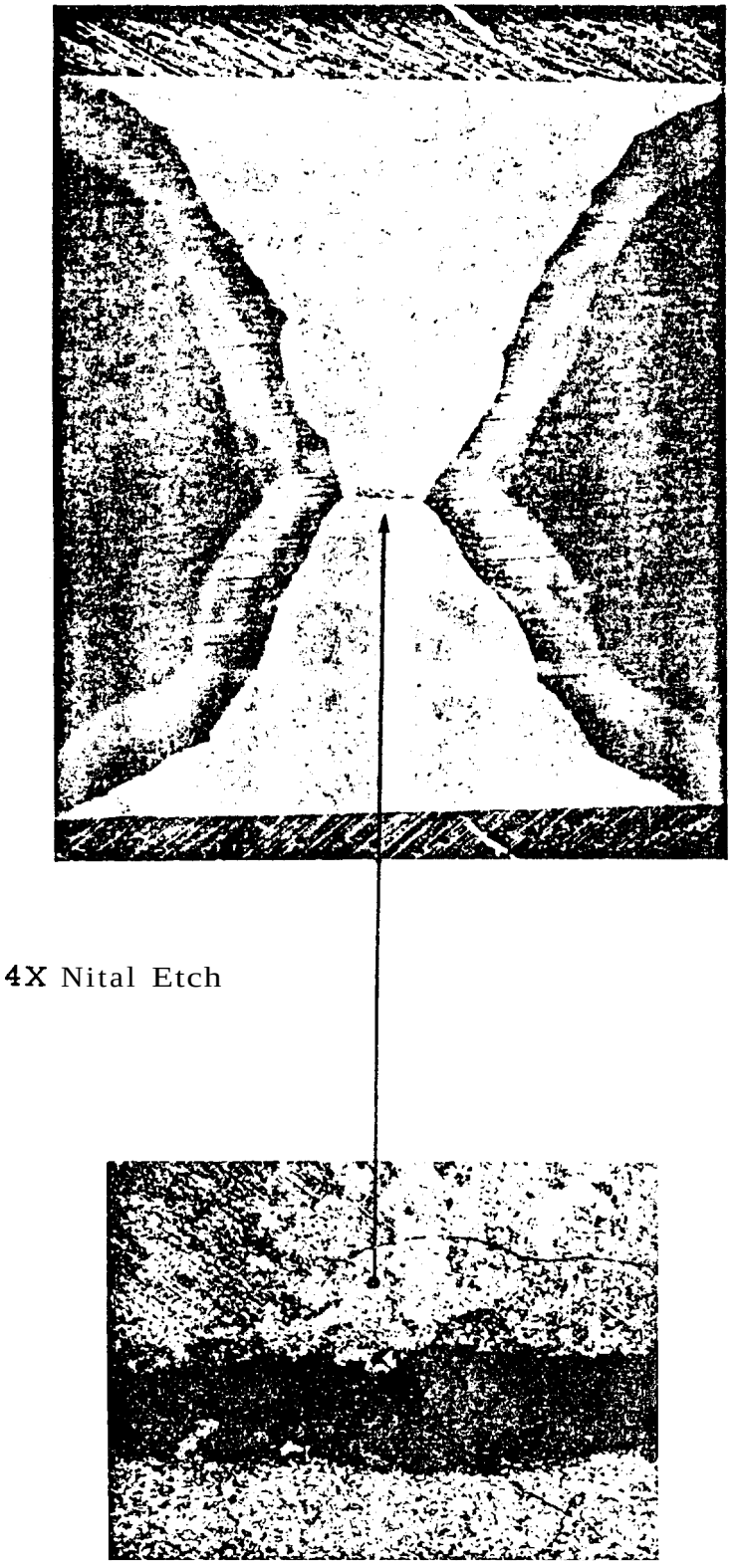

Figure *36* - The source of the indication noted at point **A of** Figure **35.** After Cross and Tooley (86).

e. Imaging

Data presentations considered in this report will be limited to those produced by conventional A, B and C-Scans. However, the accumulation and computer reconstruction of such scan data can provide a three-dimensional analysis. The basis for such displays has been reported by Watkins [20] in England (1973) and Saski [50] in Japan (1974). The systems are still in the developmental stages and have indicated encouraging preliminary results. The detection assembly is in the immersion mode and consists of a variable angle beam with a range of $\pm 70^{\circ}$ and a normal incidence longitudinal wave; both operating in the pulse-echo manner. The distance-time coordinates (X,Y) of the reflected ultrasound noted by the angle beam and/or the normal beam (Y) at a given Z coordinate are processed into a B-Scan display. At each scan point, it is necessary to determine the direction and amplitude of the refracted interrogating angle beam as well as the returning reflected components. For a given material to be interrogated such determinations are a function of the incident angle and can be accomplished by appropriate programmed computers. The spot intensity is modulated by the amplitude of the reflected ultrasound. Figures 37 and 38 indicate some experimental results obtained by Watkins. The system is being developed for remote automatic interrogations for applications in the nuclear power generating field. The data can be stored and differences between successive interrogations can be noted.

In comparing the data displays of Figures 37 and 38 with the highly sophisticated data processed images of holography and synthetic aperature it becomes apparent that the resolutions involved are quite different. The resolution of the latter are in the realm of the wavelength used since diffraction effects are involved. The resolution limits for the displays of Figures 37 and 38 are dependent upon beam width and transducer sizes. However, such displays can provide a unique contribution within the total spectrum of image forming techniques.

Perhaps a more informative approach to the displays typified by Figures 37 and 38 would be to construct a three-dimensional image by considering a collection of such displays as obtained by a variety of parallel scans. This can be accomplished by computer data processing techniques -- i.e., ultrasonic tomography.

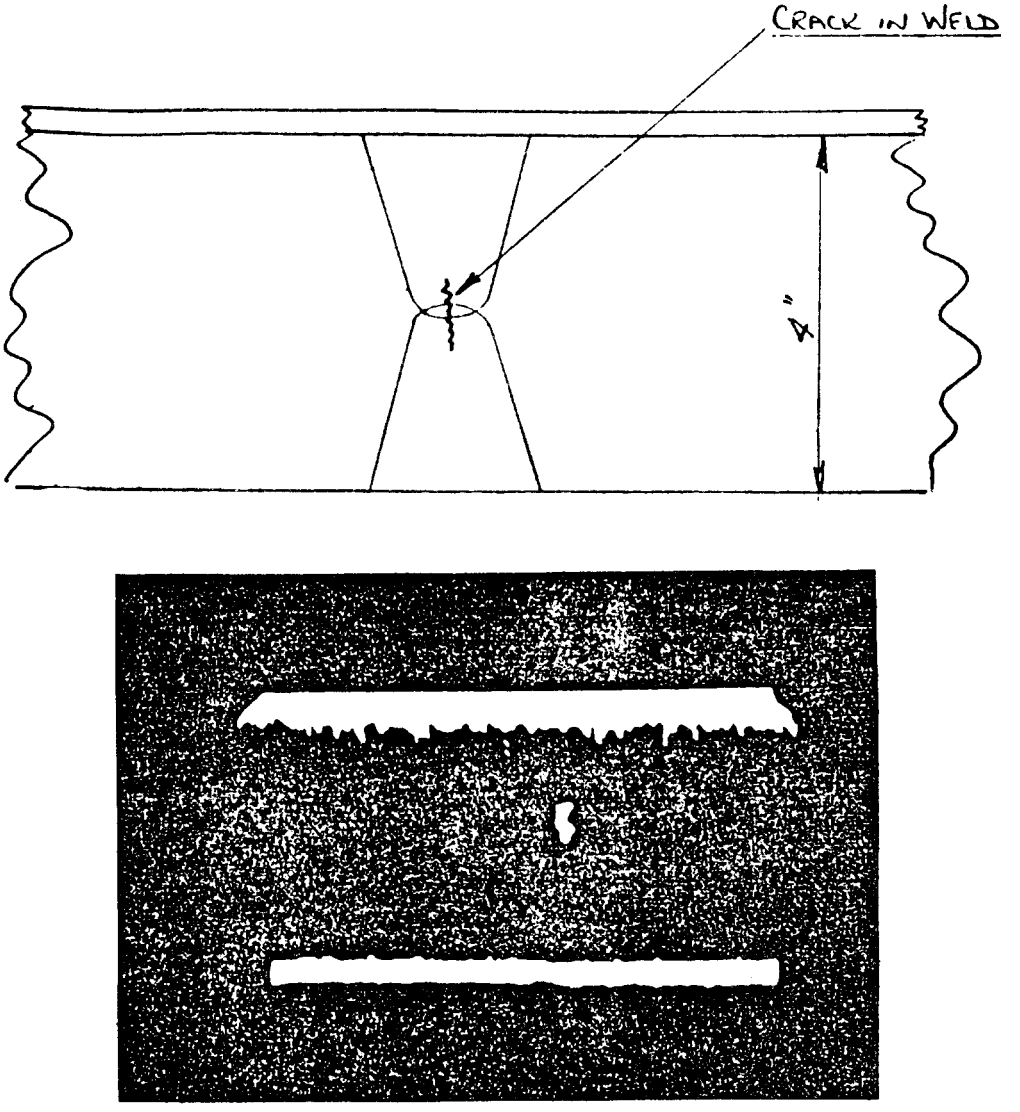

Figure 37 - A B-Scan image of a vertically oriented weld crack as generated by an angle beam sweeping ± 70° and a straight beam. After Watkins (20).

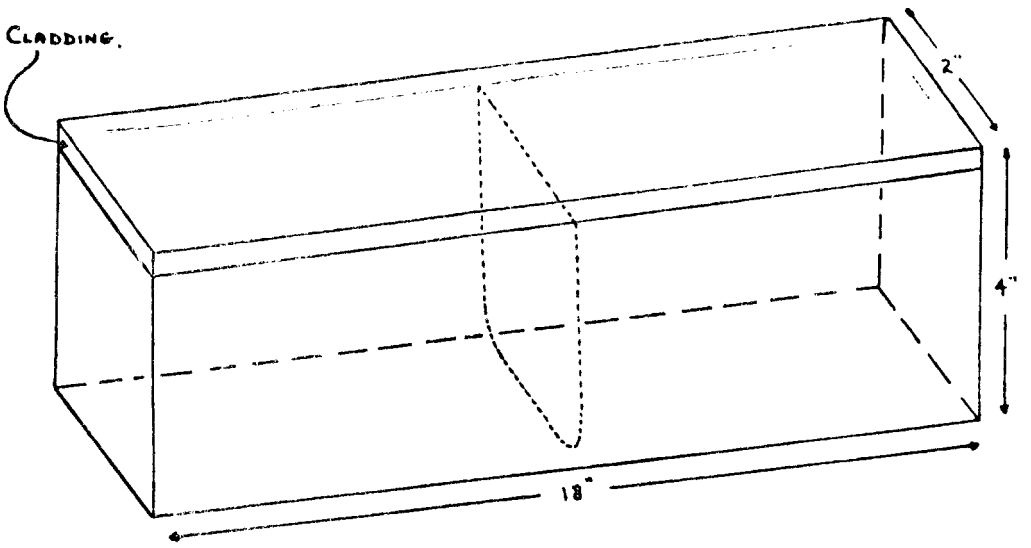

FATIGUE CRACKED TEST PIECE.

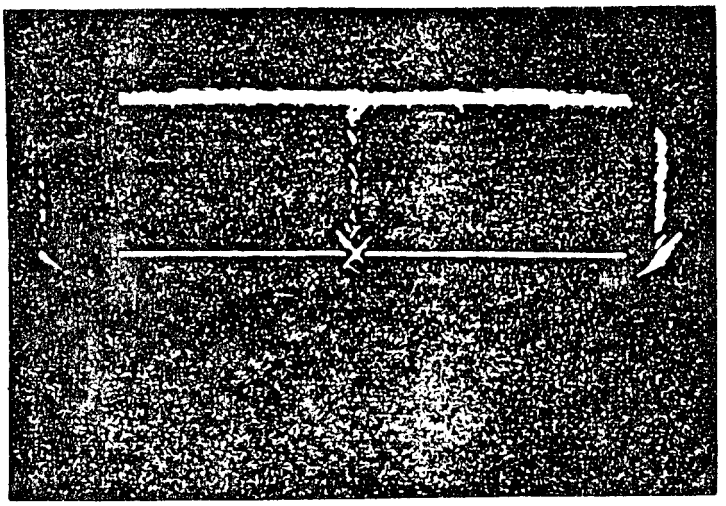

Figure 38 - A B-Scan image of a fatigue crack as generated by an angle beam sweeping ± 70° and a straight beam. After Watkins (20).

The medical field has been using ultrasonic techniques in some form since 1930. These activities are summarized in an excellent paper by Erikson et al; 376 references are listed [89]. The NDT community is slowly becoming aware of this technology and it is anticipated that a relatively considerable length of time will be required for any significant adaption of such procedures.

A novel imaging technique proposed by the Danish Welding Institute [87,88] involves a data presentation in the form of a projection of the flaw onto any desired plane within the medium being interrogated. The technique is referred to as the projection scan (P-scan). While the technique can be adapted to a number of interrogation schemes it has, thus far, been used totally for the evaluation of weldments. The elements of the instrumentation are shown in Figure 39. Attached to a conventional angle beam transducer is a cantilever beam containing a linear array of detectors. Calibration of each detector consists of its activation when it is directly over a known source of an ultrasonic indication. In the initial design, the detection was indicated by a series of light-emitting diodes. As indicated in Figure 39, this information was recorded by photographic means in a darkened area; a normal photographic exposure was also made to physically situate the flaw response to the welded structure. Figure 40 displays typical results at three different sensitivity levels. The current P-Scan equipment contains detectors which can measure the amplitude of an indication. The data is stored in a computer and later displayed at any sensitivity level. Also, the use of the computer allows the data to be reconstructed as a projection on any desired plane. Figure 41 shows the top and side projections of the flaw content of a weldment at various sensitivity levels.

It is apparent that the P-Scan provides a unique and convenient method for data presentation. It does not provide any detecting ability above that normally associated with a conventional angle beam interrogation. However, it does provide for retrieval procedures for conventional scan data to facilitate on-line or subsequent analyses; also see Section VI.

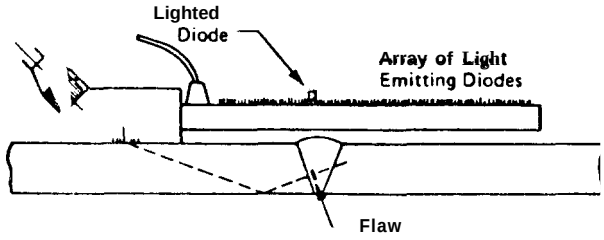

a. **Detail of Apparatus**

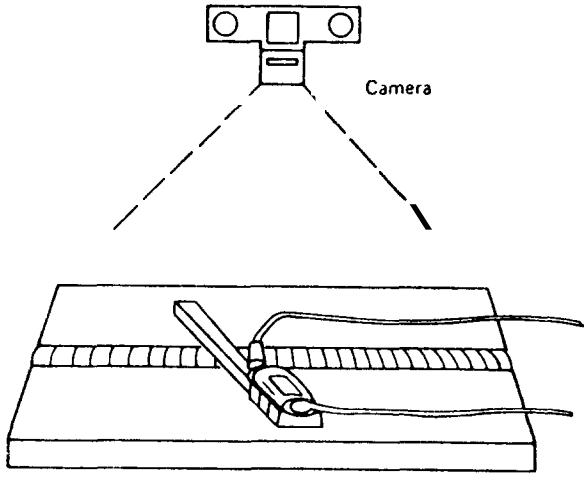

b. **Typical Recording Configuration**

Figure **39** - Projection scan system with a photographic presentation. After Lund and Jensen **(87).**

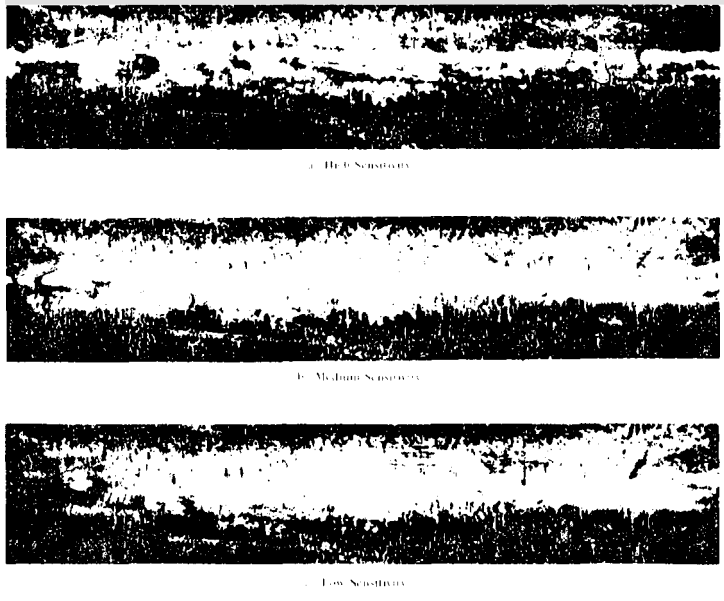

Figure 40 - Photographic Presentations of a projection scan of a weld at various sensitivity levels. After Lund and Jensen (87).

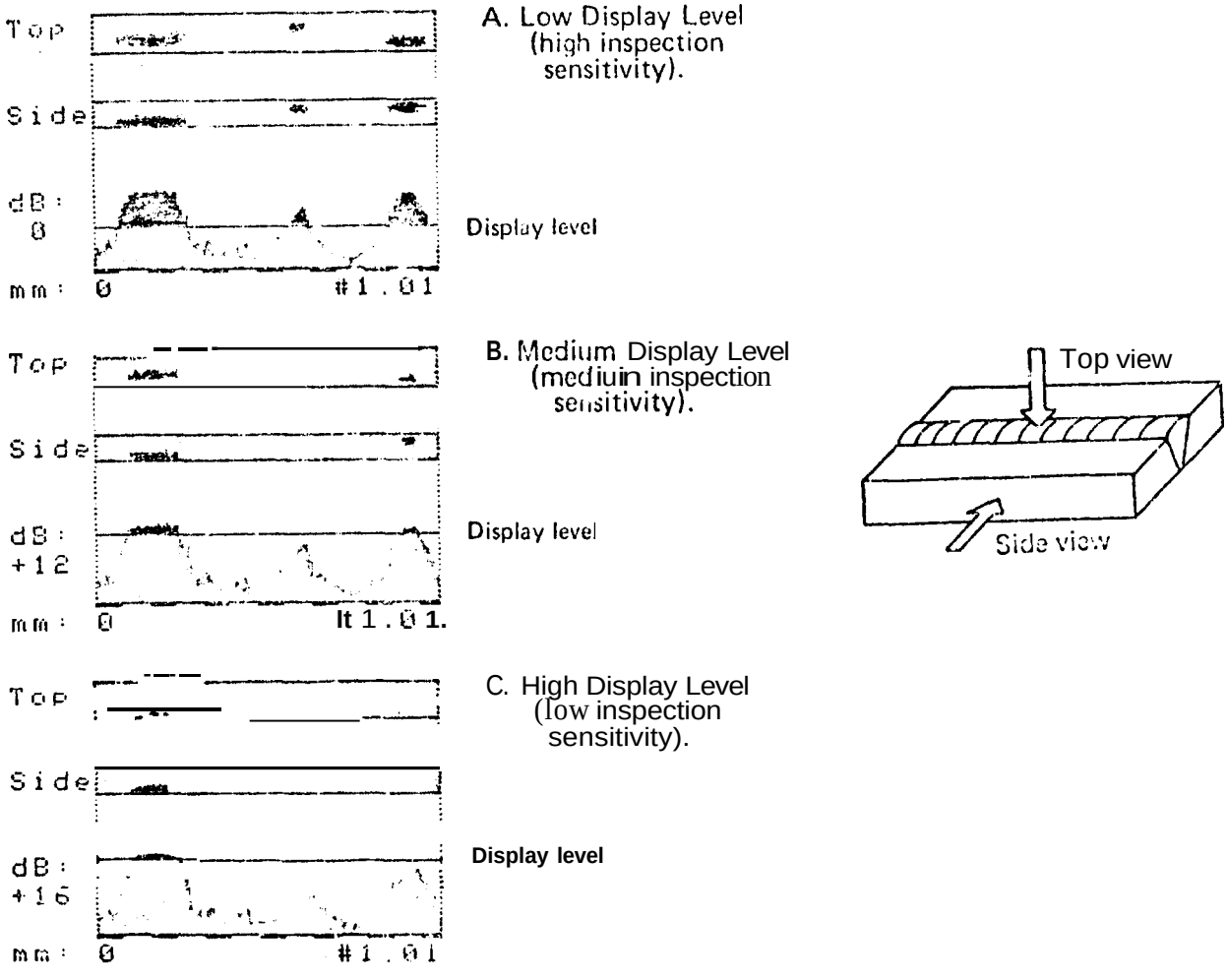

Figure 41 - Computer display of P-Scan results at three different sensitivitv levels. Danish **Welding Institute - 78.101.**